Journal of Energy Challenges and Mechanics

ISSN 2056-9386

http://www.nscj.co.uk/JECM/

Volume 4, Issue 1
April 2017

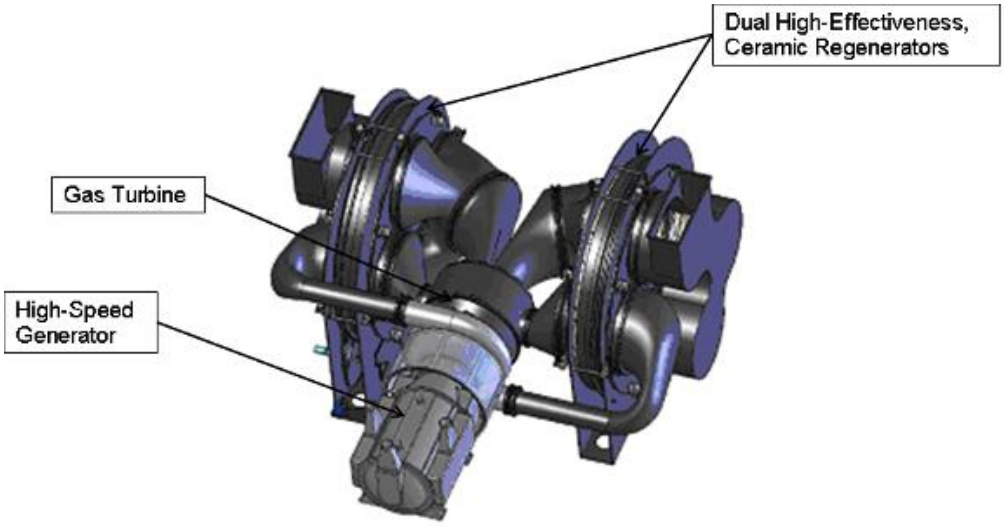

Featured article:

Distributed energy via high-efficiency ceramic gas turbines fueled by 25-MW wind turbines in the "Roaring Forties"

David Gordon Wilson
Department of mechanical engineering, Massachusetts Institute of Technology, Cambridge MA, U.S.A.

North Sea Conference & Journal LTD
2 Charlestown Walk, Cove Bay, AB12 3EZ, Aberdeen, Scotland, United Kingdom
http://www.nscj.co.uk/JECM/ | jecm@nscj.co.uk | +44(0)1224 875635

Journal of Energy Challenges and Mechanics
http://www.nscj.co.uk/JECM/
ISSN 2056-9386
Volume 4 (2017) issue 1

TABLE OF CONTENTS pages

Journal of Energy Challenges and Mechanics
http://www.nscj.co.uk/JECM/
ISSN 2056-9386
Volume 4 (2017) issue 1

Journal of Energy Challenges and Mechanics
http://www.nscj.co.uk/JECM/

ISSN 2056-9386
Volume 4 (2017) issue 1, article 1

Lessons from Living Systems for the Development of Sustainable Industrial Resource Networks

可持续工业资源网络之发展生存系统带来的启示

John Reap[1*], Astrid Layton[2]

[1]*School of Engineering, Quinnipiac University, Hamden, CT 06518, USA*
[2]*Mechanical Engineering, Texas A&M University, College Station, TX 77843, USA*

john.reap@quinnipiac.edu

Accepted for publication on 18th March 2017

Abstract - **From de Mestral's hook-and-loop fasteners to the industrial symbiosis in Kalundborg, Denmark, organisms and ecosystems have provided inspiration for multiple novel inventions. Bio-inspiration at the industrial system scale can reduce energetic and material environmental burdens as documented in the case of Kalundborg's symbiosis. Practical successes with symbioses suggest the value of ecological guidance, but a systematic means of designing ecological inspiration into an industrial resource network requires further development. Additionally, a theoretical basis for the observed environmental efficiencies needs additional elucidation. This work further develops a systematic means of using bio-inspiration in resource network design, and it explores a potential thermodynamic foundation for energetic and material efficiencies noted in industrial resource networks.**

Using an established correlation between a measure of ecological structure and 1st Law Efficiency, this work explores a theoretical basis in classical thermodynamics for observed environmental efficiencies in symbioses. Increasingly complex variations of Rankine and Brayton power cycles are analyzed in the traditional sense to determine theoretical 1st Law efficiencies. Then, they are analyzed as ecosystems using ecosystem metrics. Power cycles with increasingly ecological values for linkage density (L_d), an ecosystem network metric, are seen to possess generally higher thermodynamic efficiencies.

Moving from analysis to design, this work reports upon ongoing efforts to use ecological metrics as a guide for designing more energetically efficient, sustainable industrial resource networks. Design of a carpet tile production, reuse, and recycling network serves as an example. Using ecological metrics with target values obtained from the study of ecosystems, the structure of a modeled carpet tile network is adjusted to become more quantitatively ecological. More ecological network configurations, as measured in terms of linkage density (L_d), generate lower environmental impacts. The influence of other ecological metrics is also explored.

Keywords - **symbiosis, eco-industrial park, bio-inspiration, holistic biomimicry, biomimetic, energy.**

I. INTRODUCTION

From de Mestral's hook-and-loop fasteners (i.e. Velcro) to Kalundborg, Denmark's symbiosis (an aggregation of production facilities that use wastes as inputs), organisms and ecosystems have provided inspiration for multiple novel inventions [1]. Bio-inspiration at the industrial system scale can reduce energetic and material environmental burdens as documented in the case of Kalundborg's symbiosis [2, 3]. These industrial symbioses, also known as eco-industrial parks (EIP), contain co-located facilities that use waste material and energy from some facilities as production inputs for others, thus improving material and energy efficiency. Practical successes with symbioses suggest the value of ecological guidance for enhancing environmental sustainability, but a systematic means of designing ecological inspiration into EIPs and larger industrial resource networks requires further development. Moreover, a theoretical basis for the observed environmental efficiencies needs additional elucidation. This work advances the systematic use of bio-inspiration in the design of industrial resource networks and provides continuing evidence of a theoretical foundation for the observed benefits of bio-inspiration in these networks [4].

A foundation for systematically guiding industrial resource network design using bio-inspiration exists, but it requires further development. Biomimetic principles for guiding designs toward more environmentally sustainable outcomes were drawn from a study of biological and ecological literature [5]. Made operational using a set of ecological metrics, one of these principles was applied to the design of a modeled carpet tile industrial resource network that includes manufacturing,

distribution, reuse and recycling activities [5-7]. Making the network's structure and resource flow patterns more ecological, as measured by the suite of employed metrics, decreased the network's environmental impact. Two main areas of development remain. First, presence in ecological literature and ability to adapt findings to engineering contexts served as the primary selection criteria for ecological metrics used in industrial network design. Further screening of metrics found in ecological literature may help identify the most important ones. Second, reasons for the success of these metrics rooted in something more than the biological sciences were not apparent in the carpet tile study. The holistic approach of applying an ecological pattern may bring the observed environmental benefits for any number of reasons that further investigation can identify.

The laws of thermodynamics bind all systems, including both ecological and engineering systems. The use of thermodynamic cycles, a well-studied and understood class of networks, may explain some of the trends in values observed using the suites of measures in the carpet tile study. In fact, prior work identified a relationship between one of the ecological metrics used in the carpet tile study and the 1st Law of Thermodynamics [4]. Specifically, the study reveals a positive correlation between the ecological structural metric cyclicity and thermal efficiency when one calculates the structural metric for thermodynamic Rankine and Brayton power cycles [4]. However, this initial study only examines the relationship between one of the seven structural metrics in the original carpet tile study [6]. A similar correlation might exist for other ecological metrics. The presence of such correlations would strengthen arguments for a connection between environmental performance improvements through ecological mimicry and thermodynamic efficiency.

Testing for a correlation between the full suite of previously used structural ecological metrics and thermal efficiency advances both objectives of this work. It develops the use of bio-inspiration in resource network design by evaluating the individual metrics and by testing the thermal efficiency correlation as a general method of screening ecological metrics. Additionally, it probes at the root cause of previously observed environmental performance improvements by using a test that can link said performance to well established thermodynamic laws.

II. Method of Evaluating System Structure

To accomplish these ends, this work uses the ecological structural metrics presented by Reap [6] and used by Layton and coauthors to analyze eco-industrial parks [8]. The method of applying these metrics is the one employed by Layton, Reap and coauthors [4, 7]. This larger suite of ecological structural metrics is applied to the original set of thermodynamic cycles [4].

2.1. Ecological Structural Metrics

To quantify food web (FW) characteristics, ecologists traditionally use structural metrics based on the number of species (S) in a food web as well as the directional material and energy linkages (f_{ij}) that join them [9-12]. One should note that S may represent aggregations of species known as trophic species that share the same sets of predators and prey [13]. This allows one to represent FWs as simple two dimensional arrays **[F]** of size *S* x *S* where linkage direction is entered as traveling from row to column (See Fig. 1).

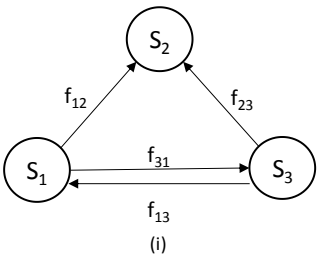

(i)

$$[F] = \begin{bmatrix} f_{11} & f_{12} & f_{13} \\ f_{21} & f_{22} & f_{23} \\ f_{31} & f_{32} & f_{33} \end{bmatrix}$$

(ii)

$$[F] = \begin{bmatrix} 0 & 1 & 1 \\ 0 & 0 & 1 \\ 1 & 0 & 0 \end{bmatrix}$$

(iii)

Fig. 1, Progression for representing a food web (FW) as a two dimensional array; (i) FW diagram; (ii) generic 2D array; (iii) 2D array for the given diagram

One uses values from and properties of this array to calculate ecological structural metrics. The sum of the directional connections in **[F]** yields a value for the number of linkages (L).

$$L = \sum_{i=1}^{m} \sum_{j=1}^{n} f_{ij} \quad (1)$$

Linkage Density (L_d) is the ratio of directional material and energy connections, links (L), in a FW to the number of species connected by the web.

$$L_d = {}^{L}/_{S} \quad (2)$$

Connectance (C_{con}) is the number of links in a FW divided by the number of possible links between species in the web.

$$C = {}^{L}/_{S^2} \quad (3)$$

Forbidding consumption within a species (cannibalism), one calculates a modified version of connectance (C_{nc}) with a smaller number of possible links.

$$C_{nc} = \frac{L}{S(S-1)} \quad (4)$$

The link structure in the food web array allows one to identify prey and predator species needed to calculate additional structural metrics. The number of prey species (n_{prey}) equals the number of nonzero rows in **[F]**.

$$f_{row}(i) = \begin{cases} 1 \; for \; \sum_{j=1}^{n} f_{ij} > 0 \\ 0 \; for \; \sum_{j=1}^{n} f_{ij} = 0 \end{cases} \quad (5)$$

$$n_{prey} = \sum_{i=1}^{m} f_{row}(i) \quad (6)$$

The number of predators ($n_{predator}$) equals the number of nonzero columns in **[F]**.

$$f_{col}(j) = \begin{cases} 1 \; for \; \sum_{i=1}^{m} f_{ij} > 0 \\ 0 \; for \; \sum_{i=1}^{m} f_{ij} = 0 \end{cases} \quad (7)$$

$$n_{predator} = \sum_{j=1}^{n} f_{col}(j) \quad (8)$$

One identifies specialized predators ($n_{s\text{-}pred}$), the number of predators consuming only one species in a web, by counting the number of columns in **[F]** with only one link.

$$f_{scol}(j) = \begin{cases} 1 \; for \; \sum_{i=1}^{m} f_{ij} = 1 \\ 0 \; for \; \sum_{i=1}^{m} f_{ij} \neq 1 \end{cases} \quad (9)$$

$$n_{s-pred} = \sum_{j=1}^{n} f_{scol}(j) \quad (10)$$

Prey-to-predator ratio (P_r) is the ratio of the number of species consumed by another species to the number of species which consume species.

$$P_r = {}^{n_{prey}}/_{n_{predator}} \quad (11)$$

Specialized predator ratio ($P_{special}$) is the ratio of the number of species that consume only one other species to the total number of species which consume other species.

$$P_{special} = {}^{n_{s-pred}}/_{n_{predator}} \quad (12)$$

Generalization (G) is the average number of prey eaten per predator in **[F]**.

$$G = {}^{L}/_{n_{predator}} \quad (13)$$

Vulnerability (V) is the average number of predators per prey in **[F]**.

$$V = {}^{L}/_{n_{prey}} \quad (14)$$

Cyclicity (λ) measures the presence and extent of cyclic pathways in a FW [14]. A value of zero for λ indicates an absence of cyclic pathways. A value of one reveals weak cycling; a value greater than one for λ indicates strong cycling. One determines cyclicity by finding the maximum real eigenvalue of a FW's adjacency matrix **[A]**, and the adjacency matrix is the transpose of **[F]**.

$$[A] = [F]^T \quad (15)$$

2.2. Ecological Metrics in Power Cycles

As a starting point for analysis, this work uses previously developed thermodynamic network representations [4]. These thermodynamic networks represent the system topology of a series of increasingly complex ideal Brayton and Rankine thermodynamic power cycles. Fig. 2 depicts the equipment present in a basic Brayton Cycle. Conversion of this diagram into an array analogous to a food web illustrates the process used for each analyzed cycle.

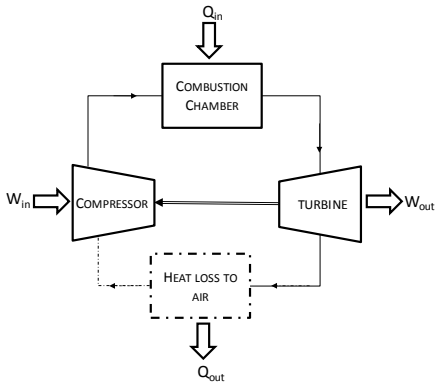

Fig. 2, Equipment diagram for a basic Brayton Cycle

The major components in each cycle's equipment diagram serve as vertices (also known as nodes) in a thermodynamic network with edges formed by flows of energy. Energy flows between vertices appear as work, heat, and working fluid containing embodied energy above that of the cycle's initial state (See Fig. 3).

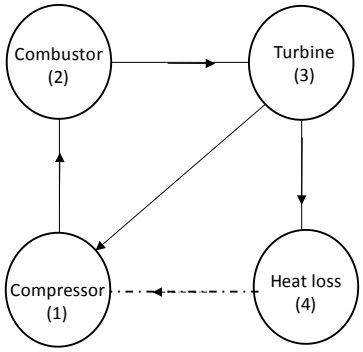

Fig. 3, Thermodynamic network diagram of Basic Brayton Cycle

One converts these network graphs to arrays analogous to food web arrays (See Fig. 4). The vertices are analogous to species (S), and the edges serve as links (L). Once converted, one calculates structural ecosystem metrics for each array.

$$\begin{array}{c} \\ 1 \\ 2 \\ 3 \\ 4 \end{array} \begin{array}{c} \begin{array}{cccc} 1 & 2 & 3 & 4 \end{array} \\ \begin{bmatrix} 0 & 1 & 0 & 0 \\ 0 & 0 & 1 & 0 \\ 1 & 0 & 0 & 1 \\ 0 & 0 & 0 & 0 \end{bmatrix} \end{array}$$

Fig. 4, Array for Basic Brayton Cycle

One compares values for the suite of structural ecosystem metrics with the classical 1st Law thermodynamic efficiencies (η_I) determined for each cycle in prior work [4] using Eq. 16.

$$\eta_I = \frac{\sum_i W_{out,i} + W_{in,i}}{\sum_i Q_{in,i}} \quad (16)$$

A simple description for each of these cycles appears in Table 1 and Table 2. Those interested in more detailed information concerning thermodynamic cycles and calculations leading to thermal efficiency should consult a thermodynamic text e.g. [15].

Table 1, Descriptions of Rankine Cycles

Rankine Cycle Description	**Cycle Name**
Basic Rankine Cycle	R1
With reheat	R2
With 1 open feed water heater (FWH) and trapped condensate	R3
With 1 open FWH	R4
With 2 open FWHs	R5
With 1 closed FWH and pumped condensate	R6
With 3 open FWHs	R7
With 1 open and 1 closed FWH	R8
With 4 open FWHs	R9
With 5 open FWHs	R10
With 6 open FWHs	R11
With 7 open FWHs	R12
With 8 open FWHs	R13
With reheat and 1 open FWH	R14
With reheat and 2 open FWHs	R15
With reheat and 3 open FWHs	R16
With reheat and 4 open FWHs	R17
With reheat and 5 open FWHs	R18
With reheat and 6 open FWHs	R19

Table 2, Descriptions of Brayton Cycles

Brayton Cycle Description	**Cycle Name**
Basic Brayton Cycle	B1
With regeneration	B2
With regeneration, intercooling, and reheat using 2 turbines	B3
With regeneration, intercooling, and reheat using 3 turbines	B4
With regeneration, intercooling, and reheat using 4 turbines	B5
With regeneration, intercooling, and reheat using 5 turbines	B6
With regeneration, intercooling, and reheat using 6 turbines	B7
With regeneration, intercooling, and reheat using 7 turbines	B8

2.3. Testing Predictions with the Carpet Tile Model

If a noteworthy correlation between thermal efficiency and an ecosystem metric appears, one expects that the correlating ecosystem metric would more substantially influence an industrial resource network's environmental performance. To test this prediction, one exercises the previously developed carpet tile manufacturing, distribution, reuse and recycling model [5, 6]. The model only needs a couple small modifications to evaluate the influence of a single structural metric instead of multiple structural and flow metrics.

The carpet tile model represents a proposed network for manufacturing, distribution, reuse, recycling and disposal of carpet tile in the metropolitan area of Atlanta, Georgia, USA. The following description is a brief overview; those seeking a detailed description are invited to consult the provided references. Steady-state material flows in the network connect a carpet tile producer, consumers, reuse centers, recycling centers and landfills for Atlanta's 13 county metropolitan region. Though steady in time, material flows and network structure can change with the design of the network. A designer can choose to send waste carpet tile from each county to either reuse or recycling centers. This choice creates a design vector of 26 variables, two flows of potentially recoverable waste carpet tile for each of the 13 counties. One uses the chosen values for each of these independent variables to solve the material flow network from which one calculates all of the discussed metrics. In the original model, these directed flows can vary from zero to the capacity constraint of the link. If set to zero, a link ceases to exist, changing the network's structure as well as its flow regime.

Exercising the model for a design vector generates values for traditional (Z_{trad}) and bio-inspired (Z_{bio}) objective functions. Smaller values for Z are associated with designs closer to the desired goals for the network. The traditional objective function consists of metrics for monetary cost (C) and environmental emissions (E_i) normalized by goal values. Environmental emissions include CO_2, SO_2, Pb, etc. Goal constants appear with g subscripts in the following equations. All of the normalized values receive equal weighting (w_{trad}) as seen in Eq. 17.

$$Z_{trad} = w_{trad}\left[\left(1-\frac{C_g}{C}\right)+\sum_{i=1}^{12}\left(1-\frac{E_{i,g}}{E_i}\right)\right] \qquad (17)$$

In the original model, a similar arrangement generates Z_{bio} (See Eq. 18). However, ecological structural and flow metrics take the place of cost and emissions. Section 2.1 introduced the structural metrics found in Eq. 18. Cycling Index (CI) and Path Length (P_L) are flow metrics which are not the focus of this work. The weighting for each metric can be set via $w_{bio,I}$ by choosing a value between 0 and 1, such that they equal one when summed. In the original model, all weights equal 1/9.

$$Z_{bio} = w_{bio,1}\left(1-\frac{L_d}{L_{d,g}}\right)+w_{bio,2}\left(1-\frac{C_{con}}{C_{con,g}}\right)+w_{bio,3}\left(1-\frac{G}{G_g}\right)+w_{bio,4}\left(1-\frac{V}{V_g}\right)+w_{bio,5}\left(1-\frac{\lambda}{\lambda_g}\right)+w_{bio,6}\left(1-\frac{P_L}{P_{L,g}}\right)+$$

$$w_{bio,7}\left(1-\frac{CI}{\mathrm{CI}_g}\right)+w_{bio,8}\left(1-\frac{\mathrm{p}_{r,g}}{\mathrm{p}_r}\right)+w_{bio,9}\left(1-\frac{\mathrm{p}_{special,g}}{\mathrm{p}_{special}}\right) \quad (18)$$

Following the method used by Layton [7] to test the predictive capabilities of a thermal efficiency correlation with a single structural metric, two modifications to the original carpet tile network model are made. First, one uses a design vector with constant magnitude flow elements. This dampens the effect of changing flow amounts on Z_{trad} which allows a clearer picture of the effect caused by changes in network structure. Second, one must place all of the weight for Z_{bio} on the evaluated structural metric. The weighting for the desired structural metric would equal one while the others would equal zero.

Having executed these changes, one can evaluate the influence of a single metric on the carpet tile network's environmental performance. First, one solves the model multiple times with stochastically generated design vectors. This work uses 1,000 model runs. The randomness in the constant magnitude vectors is achieved by activating and deactivating links. This means that each element of a given design vector either takes the value of zero or its previously fixed magnitude. Then, one checks for a correlation between Z_{trad} and Z_{bio}, recalling that a single structural metric now drives Z_{bio}. A positive correlation between the two indicates that traditional environmental and cost performance relate to the selected ecological metric.

III. Results

3.1. Ecological Metrics and Thermal Efficiency

Using Eq. 1-14, this section calculates structural ecosystem metrics for each of the power cycles described in Table *1* and Table *2*. The metric values for all cycles appear in Table 3. One should note that the thermal efficiency values (η_I) found in Table 3 originate in the work of Layton and coauthors [4]; the other metrics are determined as part of this work.

A cursory review of the data set in Table *3* reveals potentially suspicious prey-to-predator ratio (P_r) values for the Rankine Cycles. P_r equals one for all of these cycles. Given the structure of the Rankine Cycle thermodynamic network, this behavior is expected. For these cycles, each component functions as both prey and predator with the exception of the first pump and the condenser. Consider the boiler in a simple Rankine Cycle. It receives high pressure working fluid from a pump while delivering high temperature, high pressure steam to a turbine. In an ecological network sense, it feeds on the pump and is fed upon by the turbine. Similarly, the turbine feeds upon the boiler and is fed upon by the condenser. The first pump supplies high pressure working fluid to the boiler, but since it only receives working fluid at its ground state, it does not receive any energetic inputs from other actors in the system. The pump serves only as prey from an ecological perspective. Conversely, the condenser receives working fluid from the turbine in a state above that of the ground state, but it does not pass any energetic inputs to other network constituents. The condenser serves only as a predator when taking an ecological perspective. The result of these interactions is that the simple Rankine Cycle contains three elements that act as predators and three that act as prey, giving a prey-to-predator ratio of one. This is a pattern that repeats for the more complicated Rankine Cycles.

One sees that a similar relationship is not present for the Brayton Cycles. The large work inputs from the turbines needed to drive the compressors prevent the even balance between prey and predator elements. However, these work inputs coupled with other energetic connections to the regenerator create the constant vulnerability value observed for cycles B2-B8 in Table 3.

Table 4 lists coefficients of determination between thermal efficiency and the newly calculated structural metrics for both sets of cycles.

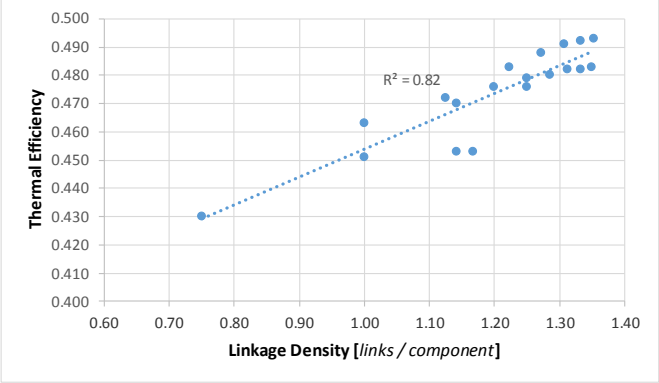

Fig. 5, Correlation between thermal efficiency and linkage density for Rankine Cycles

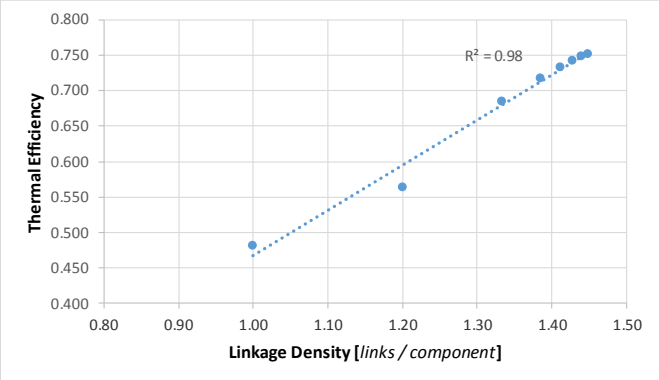

Fig. 6, Correlation between thermal efficiency and linkage density for Brayton Cycles

Table 3, provides structural metric values for Rankine and Brayton power cycles. Note that thermal efficiency values (η_I) were determined by Layton and coauthors [4]

Cycle Name	S	L	L_d	P_r	$P_{special}$	G	V	C_{con}	λ	η_I
R1	4	3	0.75	1.00	1.00	1.00	1.00	0.19	0.00	0.430
R2	5	5	1.00	1.00	0.75	1.25	1.25	0.20	1.00	0.451
R3	6	7	1.17	1.00	0.60	1.40	1.40	0.19	1.00	0.453
R4	6	6	1.00	1.00	0.80	1.20	1.20	0.17	1.00	0.463
R5	8	9	1.13	1.00	0.71	1.29	1.29	0.14	1.15	0.472
R6	7	8	1.14	1.00	0.67	1.33	1.33	0.16	1.17	0.453
R7	10	12	1.20	1.00	0.67	1.33	1.33	0.12	1.21	0.476
R8	8	10	1.25	1.00	0.71	1.43	1.43	0.16	1.32	0.476
R9	12	15	1.25	1.00	0.64	1.36	1.36	0.10	1.24	0.479
R10	14	18	1.29	1.00	0.62	1.38	1.38	0.09	1.25	0.480
R11	16	21	1.31	1.00	0.60	1.40	1.40	0.08	1.26	0.482
R12	18	24	1.33	1.00	0.59	1.41	1.41	0.07	1.27	0.482
R13	20	27	1.35	1.00	0.58	1.42	1.42	0.07	1.27	0.483
R14	7	8	1.14	1.00	0.67	1.33	1.33	0.16	1.27	0.470
R15	9	11	1.22	1.00	0.63	1.38	1.38	0.14	1.36	0.483
R16	11	14	1.27	1.00	0.60	1.40	1.40	0.12	1.39	0.488
R17	13	17	1.31	1.00	0.58	1.42	1.42	0.10	1.40	0.491
R18	15	20	1.33	1.00	0.57	1.43	1.43	0.09	1.41	0.492
R29	17	23	1.35	1.00	0.56	1.44	1.44	0.08	1.41	0.493
B1	4	4	1.00	0.75	1.00	1.00	1.33	0.25	1.00	0.482
B2	5	6	1.20	0.80	0.80	1.20	1.50	0.24	1.22	0.563
B3	9	12	1.33	0.89	0.67	1.33	1.50	0.15	1.39	0.685
B4	13	18	1.38	0.92	0.62	1.38	1.50	0.11	1.46	0.718
B5	17	24	1.41	0.94	0.59	1.41	1.50	0.08	1.50	0.733
B6	21	30	1.43	0.95	0.57	1.43	1.50	0.07	1.52	0.742
B7	25	36	1.44	0.96	0.56	1.44	1.50	0.06	1.53	0.748
B8	29	42	1.45	0.97	0.55	1.45	1.50	0.05	1.54	0.751

Table 4, Coefficients of determination between thermal efficiency and the stated structural metric for each cycle

	Coefficient of Determination (R^2)	
Metric	*Rankine*	*Brayton*
Linkage Density (L_d)	0.82	0.98
Prey-to-predator ratio (P_r)	NA	0.99
Specialized predator ratio ($P_{special}$)	0.65	0.98
Generalization (G)	0.66	0.98
Vulnerability (V)	0.66	0.62
Connectance (C)	0.70	0.93

3.2. ECOLOGICAL METRICS AND ENVIRONMENT

This section presents correlations between the carpet tile model's environmental performance (Z_{trad}) and structural metrics. Plots focus on metrics predicted to correlate by the prior section's thermodynamically rooted analysis. In all cases where correlations between Z_{trad} and Z_{bio} appear, the independent variable is a normalized form of one of the previously mentioned ecological metrics. When used as an independent variable, each normalized metric receives 100% weighting in Z_{bio}.

The plots in Fig. 7 and Fig. 9 represent variation in environmental performance of the carpet model with changes in linkage density and cyclicity, respectively. The normal probability plot in Fig. 8 is present as a check of the normality assumption underlying the curve fit in Fig. 7. Coefficients of determination in Table 5 summarize findings for the relationships between Z_{trad} and metrics not predicted to correlate by the prior thermodynamic analysis. The only exception to this is Cycling Index (CI), a flow metric introduced for purposes of comparison.

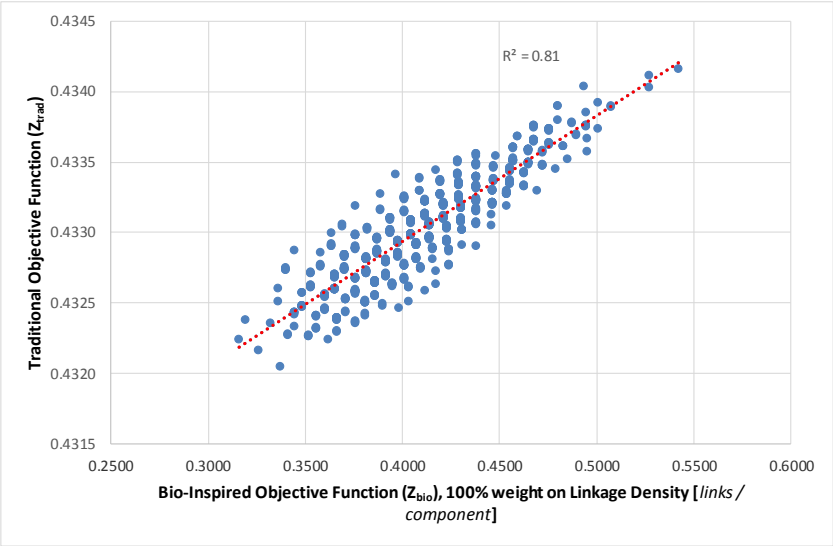

Fig. 7, Correlation between the carpet model's traditional objective function (Z_{trad}) and the bio-inspired one (Z_{bio}) when linkage density (L_d) receives 100% weight; plot based on 1000 randomly generated design vectors

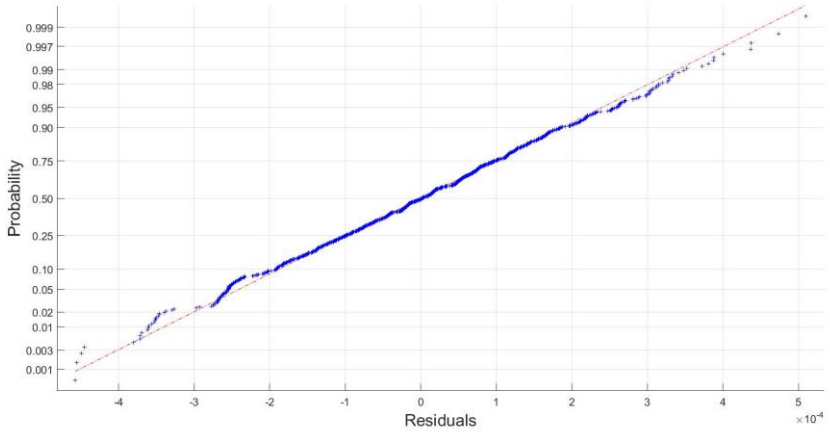

Fig. 8, Normal probability plot for data in Fig. 7

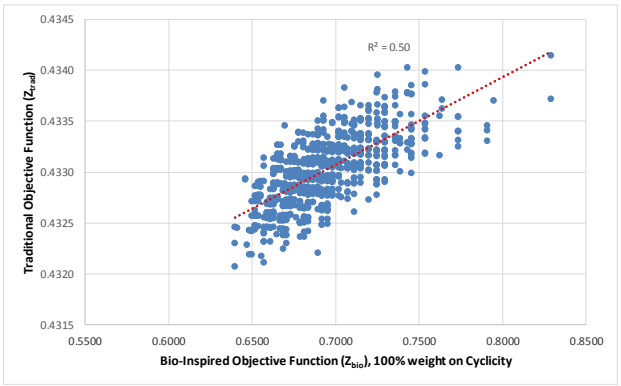

Fig. 9, Correlation between the carpet model's traditional objective function (Z_{trad}) and the bio-inspired one (Z_{bio}) when cyclicity (λ) receives 100% weight; plot based on 1000 randomly generated design vectors

Table 5, Coefficients of determination between Z_{trad} and Z_{bio} achieved when listed ecological metrics receive 100% weight; based on 1000 randomly generated design vectors

Metric with 100% Weight in Z_{bio}	**Coefficient of Determination (R^2)**
Prey-to-predator ratio (P_r)	0.62
Specialized predator ratio ($P_{special}$)	0.52
Generalization (G)	0.80
Vulnerability (V)	0.22
Connectance (C)	0.02
Cycling Index (CI)	0.96

IV. Discussion

4.1. Clarity Among Thermodynamic Correlations

One may infer the thermal efficiency (η_I) of Rankine and Brayton power cycles from linkage density (L_d). For the analyzed cycles, the most robust relationship between the newly calculated structural metrics and thermal efficiency occurs with linkage density (See Fig. 5 and Fig. 6). The coefficient of determination (R^2) between the two reaches 0.82 for the Rankine Cycles and 0.98 for the Brayton Cycles (See Table 4). This level of correlation corresponds to that determined by Layton and coauthors when comparing cyclicity with thermal efficiency for these cycles [4]. They concluded, "…the structural method for computing energy cyclicity accurately predicts maximum thermal efficiency…" for these cycles [4]. This work suggests that one may add linkage density as a predictor of maximum thermal efficiency.

The value of comparing structural metrics with thermal efficiency across multiple cycle types became apparent during this analysis. Viewing only coefficients of determination for Brayton Cycles in Table 4, one would conclude that all structural metrics except vulnerability possess predictive power. Further comparison with Rankine Cycle correlations reduces the viable metrics to linkage density. Correlations with the carpet tile model in Table 5 reinforce the finding that many of the other structural metrics only weakly associated with environmental impact. From a mathematically mechanical point of view, the substantial thermodynamic work flows from the turbines to the compressors increase the number of connections in the Brayton Cycle FW arrays. The increased number of connections and the cyclic paths which form as a result appear to enhance the correlations. If one takes a more philosophical view of the correlation differences between cycles, interesting questions emerge. Is one type of cycle more appropriate for identifying a connection with thermal efficiency? The perspective taken thus far is that a composite is more informative. Would the observed correlations hold for variants of other thermodynamic power cycles such as Otto, Diesel, Sterling, etc.? What findings might emerge from exploration of refrigeration cycles; would correlations with coefficient of performance surface?

4.2. Reflections on Carpet Model Correlations

Application of thermodynamic cycle correlations to the carpet tile model contains some surprises. Thermodynamic correlations indicate that improving cyclicity and linkage density should improve environmental performance (Z_{trad}) of the carpet tile network. The expected positive correlation (R^2 = 0.81) between linkage density and environmental performance appears in Fig. 7. However, cyclicity only weakly correlates (R^2 = 0.50) with environmental performance (See Fig. 9). As predicted, most of the other structural metrics in Table 5 exhibit weak relationships with Z_{trad}, but generalization displays a surprisingly strong correlation (R^2 = 0.80).

The correlation between Z_{trad} and linkage density is the strongest observed for the structural metrics despite indications that the selected simple linear fit may be less than ideal. This outcome aligns with expectations based on thermodynamic analysis. The normal probability plot in Fig. 8 displays a degree of nonlinearity. This suggests that the residuals may result from something other than normally distributed error and that a better curve fit is possible [16]. One should consider the purpose of such a fit, though. Curve fitting serves as a simple screening tool in this work; it identifies obvious relationships between selected metrics. The simple fit satisfies this role.

Cyclicity's weak correlation surprises for two reasons. A system needs a cyclic structure to reuse materials and energy. A system achieves lower environmental impacts if it establishes and uses its capacity to reuse resources. Since cyclicity measures the extent of a system's cyclic structure, one expects that environmental impact would correlate. The carpet tile network's high correlation (R^2=0.96) with Cycling Index (CI) provides the second reason. Unlike the purely structural metrics upon which this work focuses, CI is the cyclic fraction of flow through a system divided by the total flow through the system [17, 18]. It depends on cycling flow, and flow cycling cannot occur without a cyclic structure. So, one might expect high CI with high cyclicity. However, a possible explanation for both unexpected differences exists. The modeled system provides 26 different paths for reusing or recycling waste carpet tile, but not all paths deliver the same environmental benefits. Reuse paths generally save more energy and material per unit mass than recycling paths. The documented experiments randomly deactivate paths. This can generate networks with similar structural metric values, but one set of networks can possess more reuse links while the other contains more recycling links. In such instances, similar structures produce different environmental performance. The different flow regimes caused by favoring reuse over recycling would influence CI, thus allowing it to track environmental performance. The overall result is a set of networks that appear similar when viewed in terms of cyclicity but that one can differentiate with CI and Z_{trad}.

Generalization's (G) strong correlation, though not predicted, is less surprising than other findings. Generalization is the average number of prey consumed per predator. Increasing the number of counties sending material to the central recycling facility is the most obvious way to increase this value in the carpet model. This increase in recycling would lead to a reduction in overall environmental impact (Z_{trad}) by displacing virgin plastic inputs to carpet tile manufacture. From a more philosophical perspective, this find is also less than surprising. This work focuses on links between thermodynamic efficiency and network structure. However, network structures likely provide properties in addition to energetic efficiency. The ability to maintain function despite the loss of a network's edges or vertexs comes to mind. In an ecosystem, this might take the form of a predator that adapts to feed upon multiple prey. This adaptation enhances the predator's survival if a particular set of prey species disappears. The ecosystem gains alternative paths for resource flow. In an EIP, a facility might source a

particular type of waste, which it uses as an input, from multiple other EIP facilities.

4.3. Implications for Resource Network Design

From a design perspective, this work makes progress on identifying more influential metrics and on demonstrating a general method for screening metrics. It adds linkage density to the short list of metrics that bare some connection with thermal efficiency. As a result, this finding increases the importance of linkage density when designing industrial resource networks such as EIPs. However, though tempting, one should not yet embrace the idea that linkage density drives thermal efficiency or vice versa. These data present only a correlation. The old warning concerning the difference between correlation and causality still holds. Other factors apart from those measured might drive both.

Comparisons between ecological metrics and thermodynamic cycle efficiencies show some, limited promise as a screening method. Screening methods only work if they detect a difference among screened entities. Coefficient of determination values for the various metrics differ within each cycle. They differ between the two cycles as well (See Table 3). The differences prove substantial enough to sort the metrics. Furthermore, one can generate these comparisons rapidly since thermal efficiencies and cycle structures remain fixed after one models them. If one chooses to use a new metric for ecological structure, he simply draws the relevant structural data from the FW arrays for the cycles in order to calculate it. However, one should use this screening method with caution. While successfully identifying linkage density as a metric that correlates with environmental performance, it fails to spot generalization and over emphasizes cyclicity. In the very least, this indicates the need for additional means of screening metrics used in resource network design.

The noteworthy correlations between Z_{trad} and both G and CI suggest further investigation of these types of metrics. This study's method aims to detect the potential influence of the 1st Law of Thermodynamics on network structure. Generalization's (G) value may emerge from an influence on network robustness, not thermodynamic efficiency. This suggests that work on screening networks for robustness may prove beneficial. The high correlation with CI underscores the importance of flow metrics when quantifying the environmental performance of industrial resource networks. Investigating the underlying causes of this connection should prove fruitful.

4.4. On Thermodynamic Foundations

Whether ecological or industrial, thermodynamic laws bind resource networks. The hypotheses of this work are that industrial resource networks possess structural differences related to 1st Law Thermodynamic efficiencies and that these differences translate into differences in environmental performance. The power cycle correlations in Table 4 coupled with findings in earlier work [4] reveal that some metrics of ecological structure appear to possess a relationship with 1st Law thermal efficiencies. The results presented in Section 3.2 and discussed in Section 4.3 show that this relationship does not always translate into differences in environmental performance, though.

Generalization appears unimportant from a thermodynamic perspective, but it correlates well with environmental performance in the carpet model. However, one should not expect every important network property to correlate with just one physical principle. The unexpected value of G argues less against a thermodynamic explanation as for the influence of other principles.

Cyclicity's lack of correlation presents a more difficult problem. This outcome suggests that thermal efficiency relationships hold limited power of prediction. This, in turn, weakens any arguments for a thermodynamic foundation for observed environmental performance. As a counter, the fault may rest with the type of relationship between cyclicity and environmental performance, not the presence. Rationally, one knows that cyclic networks must exist to reuse materials and energy. Reuse lowers environmental impacts by preventing inputs of new materials. The thermodynamic correlation may simply indicate that cycles are important or that the relationship is highly nonlinear.

V. Closure

The presented work sought to achieve two goals. First, it is meant to advance bio-inspiration in resource network design by enhancing understanding of metrics previously used for this purpose. Second, it explores a potential link between environmental improvements gained through bio-inspired resource network changes and well established thermodynamic theory.

With regard to advancing bio-inspiration in network design, this work identifies a structural metric, linkage density (L_d), that correlates with thermal efficiency for Brayton and Rankine power cycles. This metric is further shown to correlate with improved environmental performance. Earlier research suggested the potential for using thermodynamic cycles to identify environmentally noteworthy network metrics. Results presented in this work provide a better understanding of the potential and limitations of using thermodynamic cycles to screen metrics for resource network design. This new evidence suggests that cycle correlations can identify important metrics. However, one cannot rely upon cycle correlations to identify all metrics with influence on environmental performance. As suggested by the case of the generalization (G) metric, other principles may explain environmental performance correlations with network metrics that fail to correlate with thermal efficiency. Principles related to network robustness and resilience deserve particular attention in future investigations.

At this point, one cannot draw a durable conclusion concerning a thermodynamic foundation. Generated information argues both for and, potentially, against the presence of such a foundation. Analysis of more thermodynamic cycles as well as more industrial resource models will provide additional, needed evidence.

REFERENCES

[1] (2016). *History of Velcro® Brand and George de Mestral*. Available: http://www.velcro.com/about-us/history#.U2o3SfldV8E.

[2] M. R. Chertow and D. R. Lombardi, "Quantifying economic and environmental benefits of co-located firms," *ES&T*, vol. 39, pp. 6535-6541, 2005.

[3] N. B. Jacobson, "Industrial symbiosis in Kalundborg, Denmark - A quantitative assessment of economic and environmental aspects." *J. Industrial Ecology*, vol. 10, pp. 239-255, 2006.

[4] A. Layton, J. Reap, B. Bras and M. Weissburg, "Correlation between Thermodynamic Efficiency and Ecological Cyclicity for Thermodynamic Power Cycles," *PLoS ONE*, vol. 7, 2012.

[5] J. Reap and B. Bras, "A Method of Finding Biologically Inspired Guidelines for Environmentally Benign Design and Manufacturing," *J. Mechanical Design*, vol. 136, pp. 11, 11/2014, 2014.

[6] J. Reap, "Holistic Biomimicry," *PhD Dissertation in Mech. Eng.*, vol. 1, pp. 425, 12/2009, 2009.

[7] A. Layton, "Food Webs: Realizing Biological Inspiration for Sustainable Industrial Resource Networks." *PhD Dissertation in Mech. Eng.*, 2015.

[8] A. Layton, B. Bras and M. Weissburg, "Industrial Ecosystems and FoodWebs: An Expansion and Update of Existing Data for Eco-Industrial Parks and Understanding the Ecological Food Webs They Wish to Mimic," *J. Industrial Ecology*, vol. 20, pp. 85-98, 2015.

[9] F. Briand, "Environmental Control of Food Web Structure," *Ecological Society of America*, vol. 64, pp. 253-263, 1983.

[10] F. Briand and J. E. Cohen, "Environmental Correlates of Food Chain Length," *Science*, vol. 238, pp. 956-960, 1987.

[11] T. H. Schoener, "Food Webs from the Small to the Large," *Ecology*, vol. 70, pp. 1559-1589, 1989.

[12] P. H. Warren, "Variation in Food Web Structure: The Determinants of Connectance," *The American Naturalist*, vol. 136, pp. 689-698, 1990.

[13] A. J. Dunne, R. J. Williams and N. D. Martinez, "Food-web structure and network theory: The role of connectance and size." *Proceedings of the National Academy of Sciences of the United States of America*, vol. 99, pp. 12917-12922, 2002.

[14] B. D. Fath and G. Halnes, "Cyclic energy pathways in ecological food webs," *Ecological Modelling*, vol. 208, pp. 17-24, 2007.

[15] Y. A. Cengel and M. A. Boles, *Thermodynamics: an Engineering Approach.* Boston: WCB/McGraw-Hill, 1998.

[16] A. J. Hayter, *Probability and Statistics for Engineers and Scientists.* Pacific Grove: Duxbury, 2002.

[17] R. R. Bailey, "Input-Output Modeling of Material Flows in Industry," *PhD Dissertation Mech. Eng.*, 2000.

[18] R. R. Bailey, J. Allen and B. Bras, "Applying Ecological Input-Output Flow Analysis to Material Flows in Industrial Systems - Part I: Tracing Flows," *J. Industrial Ecology*, vol. 8, pp. 45-68, 12/2004, 2004.

Journal of Energy Challenges and Mechanics
http://www.nscj.co.uk/JECM/

ISSN 2056-9386
Volume 4 (2017) issue 1, article 2

Distributed energy via high-efficiency ceramic gas turbines fueled by 25-MW wind turbines in the "Roaring Forties"

由25兆瓦风力发电机组驱动之高效陶瓷燃气轮机于“咆哮西风带”所生成的分布式能源

David Gordon Wilson

Department of mechanical engineering, Massachusetts Institute of Technology
Cambridge MA, room 5-324, 02139-4307, U.S.A.

dgwilson@mit.edu

Accepted for publication on 24th August 2017

Abstract: **The gas turbines are based on MIT patents that use very low cycle pressure ratios (e.g., 2.5:1) facilitated by very-high-effectiveness (e.g., 97%) regenerative heat exchangers. The low-pressure ratios are produced by compressors and turbines that have low blade speeds (e.g., 250 m/s vs. 600 m/s in "regular" designs), involving low stresses (proportional to the square of the blade speed) that permit ceramics to be reliably used in the hot-gas turbines, and that have very low noise levels (turbomachinery noise being proportional to approximately the fourth power of blade speed). A power output of 300 kW has been chosen, and the cycle waste heat can be used for building heating and cooling leading to overall efficiencies (energy used and delivered divided by energy input) around 80 percent. The energy input is initially from natural gas that can be supplemented by the infusion of hydrogen produced preferably by far-offshore wind turbines in the high-wind belt south of Australia, New Zealand and the Tierra del Fuego. A new form of turbine would be very reliable at average wind speeds of 30 m/s producing compressed hydrogen from seawater that could be delivered to pipelines up to 100-km long to which floating turbines could be connected and tethered, and the fuel could be transferred to tankers at land-based ports. These wind turbines could be as much as 25-MW capacity each, and a reasonably sized wind farm in this belt could eventually supply the energy corresponding to the entire world's 2016 usage of fossil fuels**.

Keywords: **distributed energy, ceramic hot-gas turbines, high-wind turbines, intrinsic fuel production from wind turbines**

I. INTRODUCTION

This paper may be criticized for being a shameless attempt to ask for a second look at a failed concept. However, an early failure is nowadays happily regarded as potentially excellent education. The concept is one that could claim to be capable of "saving the world" (major reduction in CO2 emissions, higher electricity-generation efficiency, and a great reduction in transmission lines), and one where the weak points of the first realization have been substantially strengthened.

The original concept for distributed energy generation through small high-efficiency gas turbines was based on two MIT patents, one being for a very-high-efficiency thermodynamic cycle[1] and the other for a very-high-effectiveness regenerative heat exchanger.[2] In combination, these could result in 300-kW generators with electrical efficiencies of 50 percent. Most distributed-energy arrangements use petrol or diesel engines that have substantially lower efficiencies, shorter lives and greater noise and pollutant emissions, so that the concept had considerable promise for taking over general electricity production. Proponents of distributed generation like to point to the switch from central large computers to individual desktop or laptop computers to forecast what is possible and likely. The 300-kW generator size is appropriate for small businesses, hospitals or groups of homes (figure 1.)

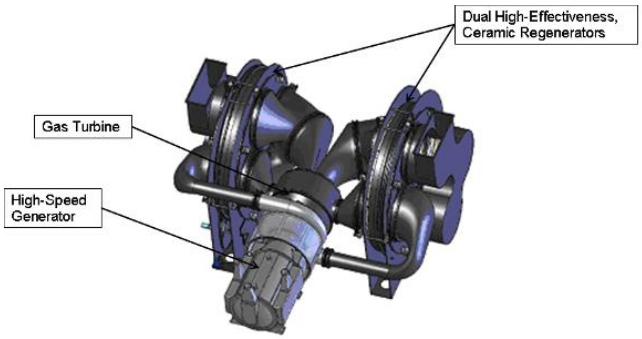

Fig.1, Wilson TurboPower 300-kW gas-turbine generator

The efficiencies of electricity "at the plug" for homes and small businesses is presently in the mid-thirties, even when the electricity is generated by 250-MW combined-cycle plants with efficiencies that may be over 60 percent. Distributed energy eliminates long cross-country transmission lines, and step-up and step-down transformers are not needed. In addition, the waste heat, 50 – 60 percent of the input energy, can be used for building heating or cooling on site. It is economic to transport waste heat only a few hundred meters, so that little of the waste heat from central plants is used, but virtually all that from distributed plants can be profitably employed. Thereby the overall energy efficiency of distributed generation can be in the seventies or eighties, and could take over electricity generation and distribution.

II. Distributed Energy

2.1. The Brayton (Joule) cycle employed

The thermodynamic cycle of the original concept was reviewed favorably by "outside" consultants (Brayton Energy, Hampton, New Hampshire) and is being retained. It has considerable advantages for distributed applications. The Brayton cycle used for aircraft and for combined-cycle gas turbines is simple, having a compressor, a combustor, and an expansion turbine. In a combined-cycle plant the compressor pressure ratio maybe thirty or forty to one, requiring expensive compressor blades and rotors running at high speeds and Mach numbers. The pressure ratio of our 300-kW compressor is 2.5:1, capable of being delivered by a small number (e.g., four) of axial-flow compressor stages running at low Mach numbers and speeds (blade speeds of about 250 m/s, versus over 600 m/s for combined-cycle plants.) The noise produced by blading is proportional to about the fourth power of blade speed, giving almost whisper quietness for the distributed-power engines. A high turbine-inlet temperature is essential for aircraft and combined-cycle turbines because it increases the thermal efficiency and reduces the turbine size simultaneously, and current values are in the region of 1650℃. The air-cooled blades are extremely expensive, and are out of consideration for the tiny turbine blades of a 300-kW engine. We are instead using ceramic blisks (combinations of blades and disks), initially in silicon carbide which were tested to run at double design speed, figure 2.

Fig. 2, Silicon Carbide turbine rotor made by Saint Gobain to Wilson TurboPower design

We would make future blisks in silicon nitride because of its much lower susceptibility to thermal-shock failure and its capability for the use of a higher turbine-inlet temperature. We are able to choose ceramics because of the very low blade speeds and consequently low centrifugal stress produced in our design. Our turbine-inlet temperature is conservatively set at 1230℃, capable of future increase in temperature and efficiency. (The lack of need for air cooling compensates somewhat for the relatively low temperature.) The three turbine stages have three identical blisks with blades shortened for the first and second stages, and a patented connection system.[3]

These small engines operate on the heat-exchanger cycle, in which the hot turbine exhaust passes through a heat exchanger that transfers heat to the compressed air leaving the axial-flow compressor, and thus reduces the gas fuel needed in the combustors. Such cycles have low optimum pressure ratios, very low for high-effectiveness heat exchangers. The effectiveness attained from our patented ceramic-honeycomb regenerators was about 0.975, far higher than the usual 0.75-0.85 for gas-turbine recuperators. However, the leakage was higher than desirable and would penalize the overall thermal efficiency of the engine. We have since patented (Ref. 4) an improved regenerator shown in figure 3 that should produce an equivalent effectiveness coupled with very low leakage.

In the original regenerator, the circular ceramic honeycomb matrix was periodically accelerated in rotation and then brought to rest so that the seals could be clamped during a short rest. In the new regenerator shown the ceramic matrix is stationary and ceramic valves periodically switch the flow

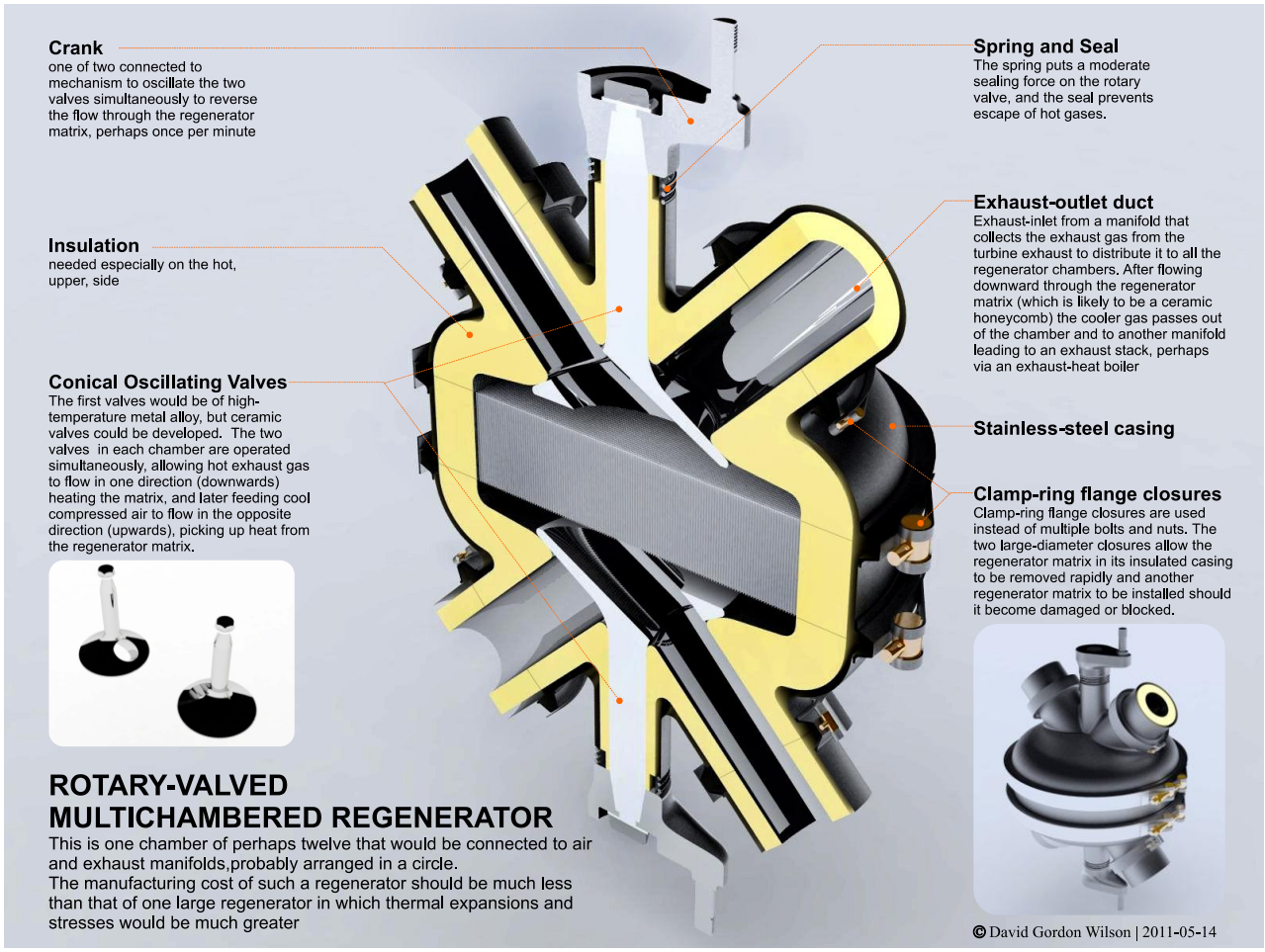

Fig. 3, Rotary-valved Multichambered Regenerator, patent 13/481,469

direction through the matrix. The cost of these small engines should be considerably below that of the central plants and distribution systems.

2.2. Gaseous Fuels

These distributed engines would use natural gas or other gaseous fuels initially, of which the world appears to have plenty. However, such fossil fuels, even though used at reduced flow rates, still contribute to global warming, and the use of "green" gases is needed in the long term. I am advocating the study of far-offshore wind in view of its outstanding apparent attractiveness.

In this I may be accused of bias, because my parents came from New Zealand. To the south of that country (and of Australia, South Africa and of the Tierra del Fuego) is a belt of the earth's surface uninterrupted by land or mountains, known as the Roaring Forties and Furious Fifties. Data on the winds in this belt are spotty, but there seems to be general agreement that the average wind speed is around 30 m/s, coming generally from the west. In most other off-shore wind areas, e.g., the North Sea, the average winds are less than half this value, under 12 m/s. The power produced by a wind turbine varies as the cube of the wind speed. The largest wind turbines presently available are rated at 8-MW, Therefore, it is possible that if one of these turbines were set up in this high-speed belt it could produce over 100 MW.

The off-shore wind technology is developing very rapidly at present (see magazines such as "Windpower" in addition to conference papers) and I am not sufficiently skilled or adventurous to forecast what might be possible in ten years. I will instead suggest that we would want to be cautious and conservative to start with and to specify that the first turbines installed should be rated at 25 MW, based on using considerably smaller turbines in this high-wind area than the largest that are available. I would also advocate developing a new type of horizontal-axis turbine that should require less maintenance than existing geared turbines, and indeed may be not maintained at all but simply replaced (see below).

Although turbine gears are being continually improved, gear failure is still a serious problem in wind turbines. Gearing is often desirable because the optimum peripheral speed of the rotor of an electrical generator is around 100 m/s. The tip-speed ratio (blade peripheral speed over wind speed) of a standard three-bladed turbine is 6-7. Therefore, in the usual wind-speeds averaging under 12 m/s the blade tips are approaching the optimum speeds. One could

simplify the generation machinery and do without the gearbox by putting iron armatures on the blade tips and have these go through magnetic fields in stationary passages (figure 4.) For three-bladed wind turbines these would need to be in two 60-degree sectors on either side of the turbine central support.

These sectors are large, and using six-bladed turbines instead of three would reduce the spread of the stator sectors considerably smaller turbines in this high-wind area than the largest that are available. I would also advocate developing a new type of horizontal-axis turbine that should require less maintenance than existing geared turbines, and indeed may be not maintained at all but simply replaced (see below).

Although turbine gears are being continually improved, gear failure is still a serious problem in wind turbines. Gearing is often desirable because the optimum peripheral speed of the rotor of an electrical generator is around 100 m/s. The tip-speed ratio (blade peripheral speed over wind speed) of a standard three-bladed turbine is 6-7. Therefore, in the usual wind-speeds averaging under 12 m/s the blade tips are approaching the optimum speeds. One could simplify the generation machinery and do without the gearbox by putting iron armatures on the blade tips and have these go through magnetic fields in stationary passages (figure 4.) For three-bladed wind turbines these would need to be in two 60-degree sectors on either side of the turbine central support.

These sectors are large, and using six-bladed turbines instead of three would reduce the spread of the stator sectors to only 30 degrees on either side of the central strut (figure 5.) The tip-speed ratio of a six-bladed rotor is about 3.5 so that the matching would again be pretty good.

Fig. 4, Three-blade no-gearbox wind turbine

I am further proposing (under the guidance of the MIT Technology Licensing Office) that the blading be stabilized by triangulated tensile cables (figure 5) to increase the accuracy of the fit of the blade tips to the channels.

Each turbine could produce electricity that could be brought to land directly, or could be converted to hydrogen or possibly to alcohol or other liquid fuel.

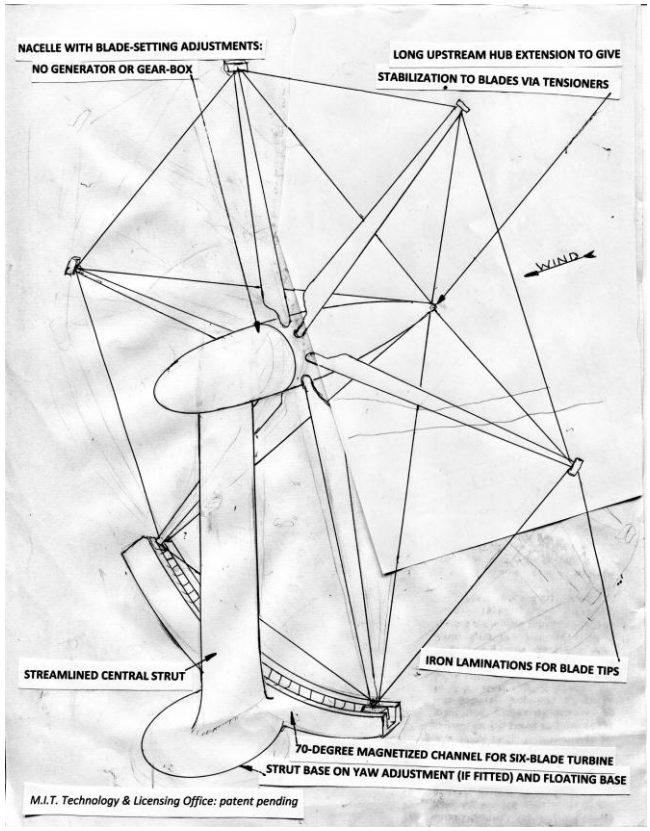

Fig. 5, Six-blade no-gearbox stabilized wind turbine

2.3. HARVESTING

The maximum economic length of a delivery conduit for electricity or hydrogen or liquid fuel from an off-shore turbine is about 100 km. We do not yet know whether the mean wind speed increases steadily as one goes south from Dunedin, NZ, or if there is a local maximum along the way, or if one reaches an economic optimum before going the full distance.

At the shore the turbines would be assembled and towed out to the selected position and erected, floating and tethered (Ref. 5) and connected to shore by the power-delivery system chosen. On-shore there would also be systems to convert the electricity to gaseous or liquid fuel and loaded on to tankers for delivery around the world. Typically, a long-distance fuel tanker uses about 2 percent of its fuel for its delivery. Others have considered shipping hydrogen, and have concluded that pure hydrogen can be injected into natural-gas pipelines with no added risks. (I would want to see this finding thoroughly checked.)

2.4. Size of Wind Farm

The US consumption of energy is about 100 quads per year. The world consumption can be guessed to be roughly 400 quads per year. One quad is 10^{15} BTU, or 1.055×10^{18} joules. If the average output of the 25-MW turbines is 20 MW, the number of turbines required to supply the whole world's present usage of fossil fuels is:

$400\times1.055\times10^{18}$ / $(20\times10^{6}\times365\times24\times3600)$ = 669,000 25-MW wind turbines

This could amount to a square array of about 817 turbines on each side.

If the turbines are spaced 400 m apart, the wind farm will be about 326 km square. This is large, but if it can supply the entire world's energy while reducing the production of greenhouse gases almost to zero it seems small. In addition, there is a strong likelihood of large increases in turbine capacity being brought about from the experiences of development.

2.5. Some Other Advantages

The death toll to birds and bats can be high around land or water-based wind turbines. In some places, human observers watch for eagles and falcons and can shut down the turbines if the birds come close. There are no known bird flight paths in the Roaring Forties, nor regular shipping lanes. This can be regarded as a substantial advantage, because concern over bird safety is very likely to increase.

If the wind is constantly westerly (perhaps with a deviation of plus or minus ten degrees), it might be possible to leave out the rotary pivot on the nacelle, thus reducing turbine cost and increasing reliability.

III. Concluding Statement

The second part of this paper, the supply of green fuel to distributed gas turbines produced by a new type and unusual location of off-shore wind turbines, is proposed as an apparently very attractive area for study. An early version has been on my energy website (LESSGOVLETSGO.org) for over ten years, apparently without producing action or comment. I would welcome feedback. It is obvious, however, that considerable prior work should be done before this concept can be seriously studied. At least a year of accurate data on wind magnitude, direction and temperature must be collected at various locations in the ''Roaring Forties." The optimum method of shipping energy from the wind turbines to shore, and then to locations around the world needs at least a preliminary decision. The "triangulated" wind turbine should be examined to choose whether to use radial blades and angled tension wires or angled blades and radial tension wires. If six blades have economic advantages over three blades should nine or ten be considered? We know that the aerodynamic efficiency decreases with an increase in the number of blades unless a ring of de-swirl stator blades is added. Should maintenance be carried out for the wind turbines, or would substitution be better? Will fixed-direction wind turbines be economically acceptable?

References

[1] Patent US 6,681,557 B2 "Low-cost high-efficiency automotive turbines", January 27, 2004

[2] Patent US RE37,134 E "Heat exchanger containing a component capable of discontinuous movement" Apr. 17, 2001

[3] Patent 20,130,302,163 "Method and apparatus for connecting turbine rotors", November 14, 2013

[4] Patent 13/481,469 " Rotary-valved Multichambered Regenerator"

[5] Sclavounos, P. D., Lee, S., DiPietro, J., Potenza, G., Caramuscio, P., and De Michele, G., "Floating Off-shore Wind Turbines: Tension-Leg platform and taut-leg buoy concepts supporting 3-5-MW Wind Turbines", European Wind Energy Conference, Warsaw, Poland, April 2010

Journal of Energy Challenges and Mechanics
http://www.nscj.co.uk/JECM/

ISSN 2056-9386
Volume 4 (2017) issue 1, article 3

Present status of a revenue-neutral "four-E" policy on energy, employment, equality, and the environment

关于能源，就业，平等和环境的收入中立"四-E"政策的现状

David Gordon Wilson

Department of mechanical engineering, Massachusetts Institute of Technology
Cambridge MA, room 5-324, 02139-4307, U.S.A.

dgwilson@mit.edu

Accepted for publication on 27th August 2017

Abstract: **An energy policy devised in the US in 1973 has become adopted by legislators, scientists and advocacy groups in a number of different forms, most avoiding the safeguards introduced by the original developer. It seemed appropriate for these forms to be studied so that the advantages and disadvantages of the different forms could be understood and for conscious choices to be made in future.**

Keywords: **Energy Policy, Employment Equality, Universal Basic Income**

I. INTRODUCTION

This is a case study of an energy policy that has become popular in the US, being advocated by Dr. James Hansen, often called the world's leading climate scientist, and by the Citizen's Climate Lobby, a large and enthusiastic nationwide group, among many. I devised the policy in 1973, publicized it in November 1973 and presented it to the Joint Economic Committee of Congress in 1974, but lost control of it because of almost immediate plagiarism. I have continued to add improvements, but most of these have not been adopted, so that it now exists in several alternative arrangements. It seemed that a study of the present forms of the policy might be interesting and instructive.

To start with I am giving below the (later) form of the policy as sent several times to senior people in the Obama administration. None was acknowledged.

II. A FOUR-E POLICY: ENERGY, EMPLOYMENT, EQUALITY AND THE ENVIRONMENT (2010)

2.1. SUMMARY

The underlying principle of the proposed policy is to produce gradually increasing incentives for all parties in the US (and in other countries with appropriate inputs) to produce more "green" energy and less harmful pollution and to consume less fossil fuel. These incentives would come from fees put on fossil fuels and on easily measured (or fairly estimated) emissions. The fees would start at a low level and would be incrementally increased until a committee of Congress decides that the fee levels had reached an appropriate level. The fees would be entirely returned to legal adult residents of the US (say aged 17 and over) in monthly rebates transferred to their bank accounts or, for poorer people, distributed in debit cards. Thus, the policy would be progressive, whereas taxation of fossil fuels and of emissions is regressive. The rebates would be included in the evaluation of the cost of living so that there would be virtually no direct inflationary effects.

2.1. INTRODUCTION

The US government has many methods at its disposal to reduce the use of fossil fuels and to reduce pollutant emissions. One is "command and control", such as the CAFÉ (corporate average fuel-economy) standards for highway vehicles, and the banning of the sales of incandescent light bulbs. These approaches show a faith in high-efficiency technology to reduce fossil-fuel usage, even though there is a human tendency to be more wasteful when using cars and lights that use less energy, sometimes referred to as the "Prius effect". An extreme "command and control" measure

is rationing, not favored in the US. However, a near relative to rationing is the requirement that industries reduce pollutant emissions to, say, 50% of former levels, something that clearly discourages firms from reducing emissions before such mandates come into force. Another is price control, such as the price fixed for interstate sales of natural gas in the 1970s at a level that made it uneconomic to look for, produce and sell gas. This low level encouraged industries, even those having huge amounts of waste heat such as nuclear power plants, to use natural gas to heat buildings rather than use their own waste heat.

Another method used to reduce the consumption of undesirables is taxation, for tobacco and alcohol, for instances. When applied to something like petroleum in widespread use, taxation has three major disadvantages: it is highly inflationary; it takes a large amount of money out of normal circulation and transfers it to the government for possibly frivolous purposes like bridges to nowhere; and taxes are regressive, hurting the poor far more than the rich. A rather strange form of taxation is cap-and-trade, which is a complex system of taxing some pollution, replete, however, with permits to pollute freely. The Economist described a US bill as "Cap and trade, with handouts and loopholes" [i] They have, it seems, granted some rather generous concessions to Midwestern Democrats from states dependent on coal or heavy industry." This bill gave away 85% of carbon permits for nothing, with only 15% being auctioned, according to the quoted article.

The author, in debating with himself and others on which of these alternatives or some other would be most appropriate to handle energy shortages and pollution excesses, became intrigued by a variation of "the tragedy of the commons" known as "the shared-lunch syndrome". It can be illustrated by a group of twenty who eat lunch every day at the same restaurant. One day, someone says "Let's save the server writing out 20 checks. Just have her write one check and we'll divide it by 20." One of them realizes that now he can order lobster thermidor and pay only 1/20 of the difference over the cost of his usual egg-salad sandwich. Within a week, everyone has copied him. They are all saying "Why is lunch so expensive, and why am I getting so fat?"

2.3. The First Version of the Proposed Policy.

The incentives in the shared-lunch situation were so obviously negative and were so similar to the use of energy and to other aspects of life in the US that the author became concerned with the need to reverse these incentives. In 1973 he came up with something that was close to a simple reversal of the shared-lunch arrangements. A gradually increasing fee would be added to the price of petroleum and coal products. All the fees would go into an "impregnable" trust fund. At the end of every month the entire contents of the trust fund would be divided equally by the number of legal adults (say seventeen and older) in the country and an exactly identical amount would be deposited in each person's bank account. Thus, fossil fuels would become more expensive, but the average user would get a rebate that would cover the increased cost even if she or he did not reduce fossil-fuel usage or emissions. Poor people, getting the same rebate but being likely to use much less fossil fuels, would get a rebate that was larger than the added costs. The rich would, if they didn't change their purchasing patterns, be financially somewhat disadvantaged, but would have far greater freedom to change their life-styles than do the poor. They would buy everything that promised to reduce or eliminate their added fees. There would be a strong stimulus to job growth, e.g., in high-tech jobs and in highly insulating replacement windows. This policy was named the "modified free market" and "tax-pus-rebate" (later changed to "fee-plus-rebate" recognizing that taxes always go to the government, whereas a fee can have a more advantageous destination.) With regard to the trust fund, it was recognized that to have so large an amount of money that could not be raided by Congress may seem fanciful. However, if the funds were redirected elsewhere, the policy would become immediately inflationary and regressive in the same way as would carbon taxes.

The next version of this policy followed the description of it in 1974 to Senator Proxmire's Joint Economic Committee, and he pointed out that at a time when inflation was over fifteen percent, my policy would make it worse. The direct inflationary aspects were eliminated by requiring that the "basket" of goods and services used to assess inflation would be modified to include the rebates as reducing the cost of living, counterbalancing the increases from the effects of the fees. Later versions incorporated fees on emissions where these could be measured at low cost or could be fairly estimated. Poor people who are unlikely to have bank accounts could receive their rebates in debit cards, as used for poor relief in many countries. The modified free market produced by this policy could also be universal in that there would need to be no other government taxes or fees on fossil energy, with two exceptions. The Department of Defense could need to fund some fuel and energy systems that would not be produced by the free market. And if there were catastrophic events like earthquakes, tsunamis or asteroid impacts there may be need for crash programs under government financing and control.

2.4. A Modeling Table.

The accompanying table illustrates how the policy could be scheduled. Some notes on the table are the following.

1. No fees are put on fossil fuels or emissions during the six months after enactment, to allow time for preparation. This delay could be varied (by the chosen Congressional committee) to be shorter or longer.

2. After the six-month fallow period, fees on all fossil fuels are started at $1.00 per 500 MJ, which for gasoline is about 25 cents per gallon. The fee is increased by a suggested further $1.00/500MJ each quarter until two years after enactment, after which the increase would occur every six months for two years, and thereafter every year. The starting fee could be increased or decreased and its rate of increase could be speeded up or slowed down by Congress. Different starting fees and rates of change could be applied to different

fuels and emissions. The author prefers the uniform fee applied to the energy value in the fuels coupled with an additional fee on the emissions from the different fuels and power systems, being charged as in note 5 below.

3. The expected decreases in fossil-fuel use and in unemployment are from the conditions at enactment, and are simply the author's judgments.

4. There would be large savings in government expenditures on energy, environment, welfare, etc., many of which would no longer be required. No attempt to estimate these savings has been made here.

5. Either simultaneously or subsequently, fees would be required from emitters of greenhouse or toxic gases such as ozone (O3), methane (CH4), nitrous oxides (NOx) , carbon monoxide (CO) and carbon dioxide (CO2) , where they could be estimated or measured fairly and inexpensively, and the collected fees would be deposited in the same trust fund and distributed. The author has used as a starting point the fees for carbon derived from the carbon taxes in British Columbia, where a partial trial of this policy was instituted in 2008 and has achieved considerable success.

6. The carbon tax in British Columbia increased from $10 to $30 per metric ton over three years.

ESTIMATES OF EFFECTS OF A POLICY TO REDUCE FOSSIL-ENERGY USE, TO STIMULATE RENEWABLE ENERGY USE AND EMPLOYMENT IN THEM, AND TO AID THE POOR

Months after enactment	0	6-9	9-12	12-15	15-18	18-21	21-24	24-30	30-36	36-42	42-48	48-56
Energy fee, in units of $/500 MJ	0	1	2	3	4	5	6	7	8	9	10	11
Approximate fee in cents/gallon	0	25	50	75	100	125	150	175	200	225	250	275
Carbon fee, $/metric ton	0	10	11	12	13	14	15	16	18	20	22	24
Estimated % reduction in use	1	8	12	16	20	24	28	31	34	37	40	42
Energy fees/month, $B	0	13	25	35	45	53	61	68	74	80	84	90
Carbon fees/month, $B	0	1.2	1.3	1.3	1.4	1.4	1.4	1.5	1.6	1.7	1.7	1.8
Monthly rebate, $/person	0	60	112	159	200	237	268	299	327	351	371	396
Expected % decrease in unemployment	1.5	2.5	3.5	4.5	5.5	6	6.5	7	7.5	8	8	8
Gov't.distribution costs, $M/month	10	33	25	3	3	3	2	2	2	2	2	2
Govt. accreditation & anti-fraud costs	4	5	5	5	5	5	5	5	5	5	5	5
Approximate levels of fees at which alternative technologies would become viable without subsidies			Biomass, New hydro Geothermal					Offshore wind				

7. In the third line of the above table the author has shown his suggestion of a gradual increase for this fee. Data from the US Energy Information Administration were used for the most-recent year, 2010, to calculate the effects of this policy.

8. In the data quoted in 7 above, the US consumption of petroleum, natural gas and coal was given as 35 quads, 25 quads and 20 quads respectively. To estimate the carbon fee, the same US administration gave the CO2 produced by the three classes of fossil fuels as 73, 54 and 95 kg per million Btu of energy in the fuel. The results are shown in the seventh line of the table. (The fees for emissions are considered by the author as too small, but the rate used is an economic/political choice.) The carbon content of a kilogram of CO2 is 273 grams, so that the fees and rebates can be calculated. A fee for methane emissions is highly desirable. Recent research has stated that methane contribution to global warming is over eighty times that of CO2 per unit mass, and that there is much more methane emitted than was previously believed.

9. The author recommends that methane and ozone be included in this policy when better data are available.

10. The points at which other energy technologies would become viable without subsidies (in the last line) are taken from the Annual Energy Outlook, 2010 (DOE, 2010). Solar thermal and solar photo-voltaic would become viable at a higher range of fuel fees than those in this table. New technologies for these and other alternatives could bring economic viability sooner (i.e., at a lower fee level).

11. Data from the Energy Information Administration (DOE, 2009) indicate that households with an income of $40,000 would, if the members did not change their patterns of consumption, receive rebates equal to their outlays in fees. Households in the income range $15,000-$20,000 would use only 86% of their rebates to pay their fees, while households with income more than $75,000 would have fees 36% higher than the rebates they would receive.

12. This policy provides a convenient low-cost framework for achieving other social goals. As an example, the gross pollution of the land and more significantly the oceans by plastic bottles, cups and bags was considered using data from the Clean Air Council ("Wastes Facts & Figures" November 2010) for the collection and disposal of these items in the US to suggest a range of fees to be assessed (not shown here).

The proposed rise in fees was stopped at a level at which use of disposable plastic bottles was reduced by 90 percent when similar fees were added in the Republic of Ireland.

The use of water is considered to be greatly underpriced in many areas, and could also be considered for the addition of a fee and redistribution as a rebate.

Besides calculating the fee rebates per person per month based on the above data and estimates, the author has guessed at government monthly distribution, accreditation and anti-fraud costs and at likely reductions in US unemployment.

2.5. A NOTE ON INEQUALITY

Some people have objected to the favorable treatment of the poor in this policy. Since at least 1980 there has been overwhelmingly favorable treatment of the rich in the US. Ben Bernanke has recently (December 2010) drawn attention to the extraordinary level of inequality that has been reached in the US and the need to correct it. Rotman in *Technology Review* and an article in The Economist have added strong views on the subject. Gross inequality in any society promotes instability and a general malaise that can reach the rich.

2.6. INEVITABLE CONSEQUENCES OF THE PROPOSED POLICY

1. The use of fossil fuels – natural gas, gasoline, diesel and fuel oil, coal, nuclear fuel etc. – and emissions of pollutants would be gradually but strongly reduced. The one-billion dollars we formerly spent every day to buy non-US fuel would also be reduced.

2. Business in general would rejoice at the reduction in uncertainty about energy prices and, in consequence, would make vigorous plans for future developments of all kinds.

3. Inventors, entrepreneurs, individuals and companies would start projects to produce energy from wind, sun, biomass etc. and to reduce emissions in ways governed by the market, and would hire many people to work in them.

4. All these new employees would start paying taxes, reducing the country's deficit.

5. People would start buying more-efficient vehicles, using buses more, walking and bicycling when convenient, buying better home-heating systems, refrigerators et cetera.

6. Poor people would get a little richer because their energy and other expenditures would increase less than those of the rich, but they would get the same rebates. They would receive something like a guaranteed income and have greater self-pride. If the rebates continued to increase, virtually all would come off welfare.

7. The rich would pay out more than they would get in their rebates. However, they would have far more freedom than do the poor to change their life-styles. They would buy everything available to lower their fees: fuel-efficient cars, air-conditioning systems, LED lighting, photo-voltaic generators and so on.

8. Congress would have the right to roll back, stop or accelerate the increases in any of the individual fees put on energy or emissions at any time. They would be hearing cries of joy from many and of anguish from the rich. They might even receive evidence that would convince them that global warming has been exaggerated, and they might therefore decide to roll back fees. All these possibilities would be democratic applications of Congressional power if the pressures came from voters rather than from lobbyists.

9. Congress would be discouraged from advocating one technology over another, because the modified free market would work its magic.

10. The government could cease to put stimulus money from our taxes to increase employment and to decrease the use of fossil fuels etc. The deficit would drop fast.

11. Almost the only expenditure required of the government would be for the system for transferring the monthly rebates – surely a relatively low-cost operation - and a step up of enforcement on people seeking opportunities to cheat. This policy would shrink government, would provide incentives for all of us to solve problems, and would greatly reduce government expenditures. Additional data on the proposed policy can be found on the web-site lessgovletsgo.org

2.7. DIFFERENT FORMS IN WHICH THIS POLICY HAS BEEN PROMULGATED.

In March 1974, I attended a seminar at MIT by Kenneth Boulding, former president of the American Economic Association and of the American Association for the Advancement of Science. He was rather negative about the future, and I asked him if I might send him some concepts that I had come up with that could produce better projections. He agreed, and I sent this policy as it was then in addition to others. After a few weeks, a most extraordinary response came from Boulding, complimenting me and my economics and asking me to get my ideas published in top-level economics journals. I was of course delighted, and wrote several papers, all of which were rejected. Economics editors do not like getting economics advice from engineers. Eventually I lowered my sights to op-ed articles in newspapers and had two or three published. I also wrote to every member of Congress several times and to other individuals, and testified five times to Congressional committees. Accordingly, I thought that I was doing a good job at spreading the word when variations of my policy began appearing in different places. For instance, the Carter Administration came up with the "Well-Head Tax" that was almost identical to my policy in several respects, and was apparently advocated by a Harvard economics professor to whom I had sent the policy. He had replied that he liked it and that it should be tried out. (I was not given any credit for this). A large number of others claimed to have originated it, but I found rather recently that one of these was in charge of a Harvard energy-policy meeting in December 1974, and he came to see me to claim that he had dreamed up the policy before I had done so. I pointed out that his meeting occurred ten days after I had received a lot of coverage in local newspapers and after I had been interviewed on the radio about it, and he dropped his claim. This strange event changed my attitude somewhat, because people copying

from a plagiarist who has not credited his sources have considerably less blame than do those who copy from an originator and claim credit.

I would like, therefore, to come to more-recent proposals for some version of the policy. Perhaps the most noteworthy was the use of the policy by the right-leaning Liberal-Party government of British Columbia in 2008. As stated above, the fee per ton of carbon dioxide increased from $10 to $30 from 2008 to 2012. All the proceeds were fed back to people and businesses, some in the form of income-tax reductions, which is how my policy started until I realized that these do nothing for poor people. The rigid schedule of the fee increase was not my preferred approach, but the policy performed better than any competing variety from any other Canadian province, and grew more popular as time went on, so it was considered a success.

Before looking at other versions of the policy it can be stated that everyone wanted to have a gradual introduction of fees. None did anything about inflation. None had any possibility of a governing board that could increase or decrease the fees.

Rep Stark, California, introduced HR 594 in 2009 with a tax starting at $10 per ton, increasing at $10 per annum, without rebates.

Rep. Larson, CT, introduced HR 1337 in 2009 "America's Energy Security Trust Fund act" with fees starting at $15 per ton CO2 increasing at $10 per year.

Senators Cantwell (D- WA) and Collins (R-ME) introduced the Carbon Limits and Energy for America's Renewal (CLEAR) Act in December 2009. CLEAR proposed to rebate 75% of revenue directly to households. With Sen. Susan Collins' (R-ME) co-sponsorship, CLEAR began as a bipartisan proposal. I had recently written to both senators and thought that I was due some credit, but soon found that an indirect plagiarist from MIT had proposed the concept to them.

Senator Bernie Sanders joined with Senator Barbara Boxer to promote the Climate Protection Act of 2013 with fees rising from $20 to $33 per ton.

In 2015 Senator Bernie Sanders introduced the Climate Protection and Justice Act. The fee would start at $15 per ton CO2 and rise by $3.22 per ton per year until it reached $73/ton. The collected fees would be returned to households.

Senator Sheldon Whitehouse's 2014 American Opportunity Carbon Fee Act would have fees on CO2 and CH4 at $42/ton increasing by 2% per year.

Senator Bernie Sanders joined with Senator Barbara Boxer to promote the Climate Protection Act of 2013 with fees rising from $20 to $33 per ton.

2.8. COMMENT

The Economist has long been a strong advocate for direct taxation of pollutants, and I once tried to engage the present editor, then the economics editor, on the inflationary and regressive effects of such policies, without success. That all modern versions of the policy should show such lack of concern of inflation seems reactionary. To deny the peoples' representatives any control over the magnitude of the fees charged also seems to show a lack of trust. The need to promote a redress of equality and fairness is very disappointing. All these aspects of the policy seem to demand inclusion.

The note on the effects on inequality was written before the current increasing enthusiasm for a universal basic income as something that would combat poverty. The policy rebates produce something very close to this concept, which should be an added point in its favor.

REFERENCES

[i] Anon: "Cap and trade, with handouts and loopholes" *The Economist*, May 23 2009

[ii] Wilson, David Gordon: News release from MIT to Associated Press, United Press International, individual newspapers on a new energy policy, November 30, 1973 This was published in papers of December 2 and 4, 1973, and resulted in a WGBH radio interview of December 4, 1973

[iii] Wilson, David G.: Hearings before the Subcommittee on Priorities and Economy in Government of the Joint Economic Committee, Congress of the United States Ninety-Third Congress, May 20, 1974, pp39 et seq.

[iv] Anon: "We have a winner", *The Economist*, July 23rd, 2011, p. 35

[v] Litman, Todd: "Carbon taxes: tax what you burn, not what you earn" Victoria Transport Policy Institute, Victoria, BC, July 31, 2008

[vi] Wikipedia: "The U.S. Energy Information Administration (EIA) is a principal agency of the U.S. Federal Statistical System responsible for collecting, analyzing, and disseminating energy information to promote sound policy-making, efficient markets, and public understanding of energy and its interaction with the economy and the environment. EIA programs cover data on coal, petroleum, natural gas, electric, renewable and nuclear energy. EIA is part of the U.S. Department of Energy.

[vii] Hamburg, Steve, chief scientist: "Methane: The other important greenhouse gas; methane is 84x more potent than CO_2 in the short term" Environmental Defense Fund, NY, NY, November 2014

[viii] Moyers, Bill: "The rule of the rich", *Mother Jones*, February 2011).

[ix] Rotman, David "The disparity between the rich and everyone else is larger than ever in the United States and increasing in much of Europe. Why?" *MIT Technology Review*, vol. 117 no 8, Cambridge MA, 2014

[x] Anon: "Free Exchange: It is the 0.01% who are really getting ahead in America", *The Economist*, November 8, 2014, p. 76

Journal of Energy Challenges and Mechanics
http://www.nscj.co.uk/JECM/

ISSN 2056-9386
Volume 4 (2017) issue 1, article 4

Robust Nonlinear Backstepping Controller for a Tidal Stream Generator Connected to a High Power Grid

非线性鲁棒控制器反推用于发电机潮汐耦合到高功率网络中

Fabien Oculi[1*], Fabienne Floret[1], Homère Nkwawo[1], Raphaël Goma[1], Mamadou Dansoko[2]

[1] *Équipe 2ASD, Département GEII, Université Paris 13, 99 Avenue Jean Baptiste Clément, 93430 Villetaneuse, France*
[2] *Centre de Calculs, de Modélisations et de Simulations (CCMS), FST - USTTB, B.P. E 3206 Bamako, Mali*

fabien.oculi@iutv.univ-paris13.fr

Accepted for publication on 25th July 2017

Abstract - **Increasing global energy requirements and the emergence of renewable energy involve some efficient Smart Grids deployment in order to prevent disturbances that may occur on electrical grid. In recent years, to enhance the stability and the sustainability of power systems, a great deal of attention has been paid to nonlinear power controllers. Indeed, they could be used to maintain steady voltage and frequency under normal and dysfunctional operations. Among various nonlinear controllers, we have chosen in this paper to design a controller based on the backstepping method, which can apply to our dynamical system. These advantages of this procedure are the smoothness and robustness with respect to external disturbances. It will be applied to a tidal stream system connected to a high - power electrical network called infinite bus. Dynamics of angular speed, active power and terminal voltage of our system without controller have been compared to those obtained with a nonlinear backstepping controller and with a classical linear controller named AVR-PSS (Automatic Voltage Regulator - Power System Stabilizer). Simulations on a single machine connected to an infinite bus power system will prove that our backstepping controller achieves the convergence of the system states. Robustness is demonstrated in transient and permanent behaviours when occur a mechanical perturbation and short-circuit on the transmission line. Furthermore, the effectiveness of the proposed controller compared to classical controller allows overcome the stall phenomena of synchronous generators directly connected to a high power grid.**

Keywords - **High Power Network, Backstepping Control, Power Systems Stability, Robustness**

I. INTRODUCTION

Nowadays, robust nonlinear control strategies development is an important challenge to ensure the stability of interconnected generators to high power grids. Indeed, the emergence of renewable terrestrial and tidal current energies [1] leads us progressively to a reversible network in terms of production and consumption. Hence it is necessary to develop resilient Smart Grids capable of self-regulation in the event of long or short power failures. As a result our research area requires transversal skills such as mathematical modelling of complex nonlinear systems, electrical and control engineering. The direct high-power grid connection requires a permanent regulation of terminal voltage and frequency with a quick rejection of mechanical or electrical disturbances. In this context, the controller design must take into account the inherent nonlinear properties of synchronous generators. So far the linearized Heffron-Philips model of a Single Machine Connected to an Infinite Bus (SMIB) associated with an AVR-PSS had been improved and shown their efficiency only around operating points [2]. But, in effect, this control strategy could disconnect synchronous generator the power grid under severe disturbances. Until now few implementations of nonlinear controllers have been done on benchmarks. For this reason, our team has developed, simulated and implemented robust nonlinear controllers [3, 4, 5].

In this paper a nonlinear controller will be designed by a backstepping method. Next, the robustness of this controller was improved under disturbances such as short-circuit and

permanent turbine mechanical power drop - Fig. 1.

The paper is organised as follows: in Section II, we used third order dynamic model of SMIB elaborated in [6]. The advantage of this nonlinear state representation is that two state variables, relative angular speed of the generator (ω) and active power of the generator (P_e), are directly measurable. The power angle (δ) is obtained by integrating relative angular speed. The terminal voltage (V_t) of the synchronous generator is measurable and could be obtain by an algebraic equation. Our nonlinear system is already in a strict-feedback form, which allows design the backstepping control in Section IV. This method will achieve our control objectives summarized in Section III. We will check by simulations in section V our backstepping control law and compare this one with AVR-PSS controller.

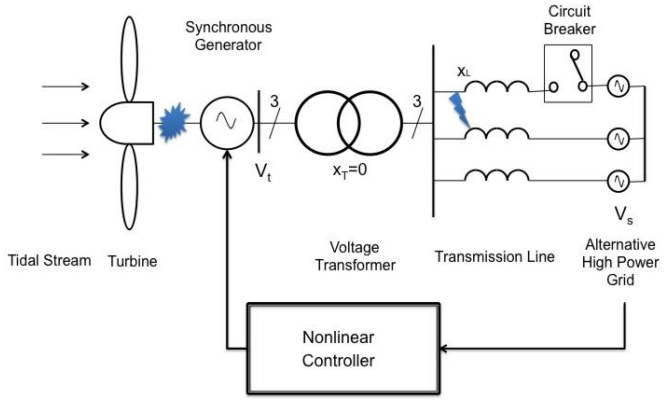

Fig 1, Tidal stream generator and his nonlinear controller connected to a high power grid

II. Problem Formulation

2.1. Assumptions

These following assumptions are based on the fact that tidal phenomena are predictable.

① The velocity of the tidal current is considered as a constant.

② The turbine mechanical power, P_m, evolves as a fast response first order system. Its steady state value is 0.8 *pu*.

③ It is assumed that all system parameters are known.

2.2. Synchronous generator dynamics model

Our nonlinear system is of the general form $\dot{x} = f(x,u)$. $x^T = [\delta\ \omega\ P_e]$ is the vector of state variables and $u = E_{fd}$ is the command. Our nonlinear system comes from formulations written in [8, 9].

$$\begin{cases} \dot{x_1} = x_2 \\ \dot{x_2} = \alpha_2.x_2 + \gamma_2 + \beta_2.x_3 \\ \dot{x_3} = x_2x_3.\cot x_1 + \alpha_3 x_2 \sin^2 x_1 + \gamma_3 x_3 + \beta_3 \sin x_1 u \end{cases} \quad (1)$$

with:

$$x_1 = \delta \qquad x_2 = \omega = \omega_g - \omega_s \qquad x_3 = P_e$$

$$\alpha_2 = -\frac{D}{M} \qquad \beta_2 = -\frac{\omega_s}{M} \qquad \gamma_2 = -\beta_2.P_m$$

$$\alpha_3 = \frac{x_d - x'_d}{x_{ds}.x'_{ds}}V_s^2 \qquad \gamma_3 = -\frac{1}{T'_{do}}.\frac{x_{ds}}{x'_{ds}} \qquad \beta_3 = -\frac{1}{T'_{do}}.\frac{V_s}{x'_{ds}}$$

$$M = 2.H \qquad x_{ds} = x_d + x_s \qquad x'_{ds} = x'_d + x_s$$

System parameters are defined in Table 1.

TABLE 1, SYSTEM-GRID PARAMETERS

Designation	Symbol	Value	Unit
Root mean square high power voltage	V_s	1	*pu*
Mechanical power turbine	P_m	0.8	*pu*
Transmission line parameters + voltage transformer			
Voltage transformer reactance	x_T	0	*pu*
Transmission line reactance	x_L	0.294	*pu*
Broken Transmission line reactance	x_s	$x_T + \frac{1}{2}x_L$	*pu*
Synchronous generator parameters			
Synchronous angular speed	ω_s	1	*pu*
Rotor angular speed	ω_g	–	*pu*
Damping constant	D	0.1	*pu*
Inertia constant	H	0.576	*sec.*
Synchronous direct axis reactance	x_d	0.894	*pu*
Synchronous direct axis transient reactance	x'_d	0.64	*pu*
Direct axis transient open-circuit time constant	T'_{do}	0.44	*sec.*

Let's write the previous system in strict–feedback form:

$$\begin{cases} \dot{x_1} = \varphi_1(x_1) + \psi_1(x_1)x_2 \\ \dot{x_2} = \varphi_2(x_1,x_2) + \psi_2(x_1,x_2)x_3 \\ \dot{x_3} = \varphi_3(x_1,x_2,x_3) + \psi_3(x_1,x_2,x_3)u \end{cases} \quad (2)$$

In our case, by identification, we have:

$$\varphi_1 = 0 \qquad \psi_1 = 1$$

$$\varphi_2 = \alpha_2x_2 + \gamma_2 \qquad \psi_2 = \beta_2$$

$$\varphi_3 = x_2x_3.\cot x_1 + \alpha_3x_2\sin^2 x_1 + \gamma_3x_3 \qquad \psi_3 = \beta_3 \sin x_1$$

$$0 < x_1 < \frac{\pi}{2}$$

2.3. Terminal voltage

Since the terminal voltage of the synchronous generator does not appear in our system Eq. (1), we get it algebraically by the following direct relation [7]:

$$V_t = \left[\left(\frac{x_sP_e\cot\delta}{V_s} + \frac{x_d.V_s}{x_{ds}}\right)^2 + \frac{(x_s.P_e)^2}{{V_s}^2}\right]^{1/2} \quad (3)$$

III. Control Objectives

Control law objectives are describe as follows:

- The power angle δ must converge to its reference value δ_{ref} define by equation Eq. (4).

- The relative speed ω of the synchronous generator must converge quickly towards zero. This means that rotor angular speed converges towards the synchronous angular speed.
- The terminal voltage of the synchronous generator V_t must converge quickly to the high power grid reference voltage V_s of 1 *pu.*

These control objectives can be summarized as follows:

$$\lim_{t \to +\infty} \begin{bmatrix} \delta \\ \omega \\ V_t \end{bmatrix} = \begin{bmatrix} \delta_{ref} \\ 0 \\ V_s \end{bmatrix}$$

with :

$$\delta_{ref} = \arccot\left[\frac{V_s}{x_s P_m}\left(-\frac{x_d V_s}{x_{ds}} + \sqrt{{V_s}^2 - \frac{{x_s}^2 {P_m}^2}{{V_s}^2}}\right)\right] \quad (4)$$

The developed control law must reject electrical and mechanical disturbances as quickly as possible.

IV. Backstepping Controller Design

Backstepping is a systematic and recursive method used to design nonlinear controllers using the second stability principle of Lyapunov. This technique was inspired by the research works of Feurer, Morse [10] in the seventies and by Kokotović and Sussmann in the eighties. Works of Krstić, Kokotović and Kanellakopoulos [11, 12] made a great contribution to the development of this technique to a very large class of nonlinear systems. The block diagram in Fig. 2 illustrates the development of the backstepping control law for our nonlinear system. This method consists in designing a controller recursively by considering state variables as virtual controls. Then, we design some intermediate virtual control laws called stabilizing functions σ_i (i = 1,2,3). This control strategy will have to achieve the objectives of stabilization and tracking of desired trajectory. For this purpose, at each step we designed control Lyapunov functions, called **clf**, including estimated states z_i also called error variables: $z_1 = x_1 - \delta_{ref}$, $z_2 = x_2 - \sigma_1$ and $z_3 = x_3 - \sigma_2$. Under the theorem of Lassalle-Yoshizawa [13] these new coordinates z_i obtained in the new state space converge asymptotically to zero - Fig 3a.

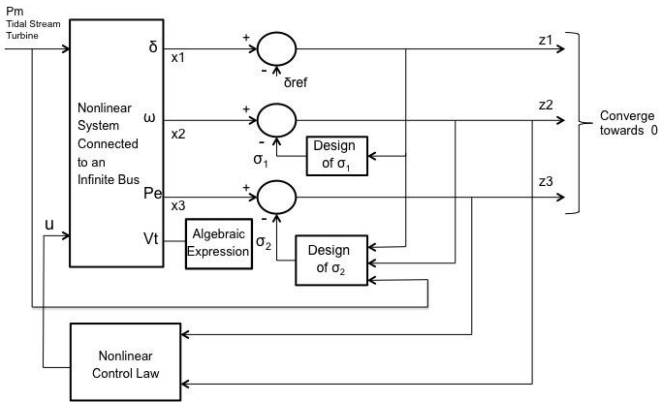

Fig 2, Block diagram of backstepping controller system

Step 1

Consider the following coordinate changes:

$$z_1 = x_1 - x_{1r} \quad (5)$$

$$z_2 = x_2 - \sigma_1 \quad (6)$$

with $x_{1r} = \delta_{ref}$ given by equation Eq. (4).

We derivate equation Eq. (5):

$$\dot{z_1} = \dot{x}_1 - \dot{x}_{1r} = x_2 \qquad (\dot{x}_{1r} = 0)$$

From Eq. (6), we get the expression of x_2 – first virtual control variable – and it is injected into $\dot{z_1}$, which gives:

$$\dot{z}_1 = z_2 + \sigma_1 \, . \quad (7)$$

Let us choose a first **clf**:

$$V_1 = \frac{1}{2} {z_1}^2$$

The time derivative of V_1 is:

$$\dot{V}_1 = z_1 . \dot{z}_1$$

We inject Eq. (7) into the previous expression:

$$\dot{V}_1 = z_1 z_2 + z_1 . \underbrace{\sigma_1}_{-c_1 z_1} \quad (8)$$

We deduce the first stabilizing function σ_1:

$$\sigma_1 = -c_1 z_1 \quad (9)$$

where c_1 is a positive constant.

Its time derivative, useful for the second step, is written:

$$\dot{\sigma_1} = -c_1 \dot{x_1} = -c_1 x_2 \quad (10)$$

Conclusion of step 1

Then the time derivative of V_1 becomes:

$$\dot{V}_1 = -c_1 z_1^2 + z_1 z_2 \, . \quad (11)$$

Clearly, if $z_2 = 0$, then $\dot{V}_1 = -c_1 z_1^2$ and $z_1$is guaranteed to converge toward zero asymptotically.

Step 2

Consider the following coordinate changes:

$$z_3 = x_3 - \sigma_2 \, . \quad (12)$$

The time derivative of Eq. (6) is:

$$\dot{z_2} = \dot{x_2} - \dot{\sigma_1} \, .$$

In the previous equation we inject the second equation of our nonlinear system Eq. (1) and Eq. (10):

$$\dot{z_2} = \alpha_2 x_2 + \beta_2 x_3 + \gamma_2 + c_1 x_2$$

From Eq. (12) we get the expression of x_3 – second virtual control variable – and it is injected into $\dot{z_2}$, which gives:

$$\dot{z_2} = (\alpha_2 + c_1) x_2 + \beta_2 z_3 + \beta_2 \sigma_2 + \gamma_2 \quad (13)$$

Let us choose a second **clf** of the form:

$V_2 = V_1 + \frac{1}{2}{z_2}^2$.

The time derivative of V_2 is:

$\dot{V_2} = \dot{V_1} + z_2.\dot{z_2}$.

We inject Eq. (13) and Eq. (11) into the previous expression:

$$\dot{V_2} = -c_1{z_2}^2 + \beta_2 z_2 z_3 + z_2[z_1 + (\alpha_2 + c_1)x_2 + \beta_2\sigma_2 + \gamma_2] \quad (14)$$

with $[z_1 + (\alpha_2 + c_1)x_2 + \beta_2\sigma_2 + \gamma_2] = -c_2 z_2$.

We deduce the second stabilizing function σ_2:

$\sigma_2 = -\frac{c_2}{\beta_2}z_2 - \frac{1}{\beta_2}z_1 - \frac{\alpha_2+c_1}{\beta_2}x_2 - \frac{\gamma_2}{\beta_2}$.

Substituting α_2, β_2 and γ_2 by their expressions we have:

$$\sigma_2 = \frac{M}{\omega_s}\left[c_2 z_2 + z_1 - \left(c_1 - \frac{D}{M}\right)x_2\right] + P_m \quad (15)$$

where c_2 is positive constant.

Its derivative, useful for the third and last step, is written:

$$\dot{\sigma_2} = \frac{\partial\sigma_2}{\partial x_1}\dot{x_1} + \frac{\partial\sigma_2}{\partial x_2}\dot{x_2}$$
$$= \frac{M}{\omega_s}[(1 + c_1c_2)x_2 + (c_1 + c_2 - \frac{D}{M})\dot{x_2}] \quad (16)$$

where $\dot{x_2}$ is the second equation of our nonlinear system Eq. (1).

CONCLUSION OF STEP 2

Then the time derivative of V_2 becomes:

$$\dot{V_2} = -c_1{z_1}^2 - c_2{z_2}^2 + \beta_2 z_2 z_3 = -\sum_{i=1}^{2} c_i{z_i}^2 + \beta_2 z_2 z_3 \quad (17)$$

Clearly, if $z_3 = 0$, we have $\dot{V_2} = -\sum_{i=1}^{2} c_i{z_i}^2$, and thus both z_1 and z_2 are guaranteed to converge to zero asymptotically.

STEP 3

In this step we will determine the control law u.

We derivate the error dynamic z_3 Eq. (12):

$$\dot{z_3} = \dot{x_3} - \dot{\sigma_2} \quad . \quad (18)$$

In the previous equation we inject the third equation of our nonlinear system Eq. (2) in which u appears:

$$\dot{z_3} = \varphi_3(x) + \psi_3(x)u - \dot{\sigma_2} \quad (19)$$

Let us choose a third **clf** of the form:

$V_3 = V_2 + \frac{1}{2}{z_3}^2$.

The time derivative of V_3 is:

$\dot{V_3} = \dot{V_2} + z_3.\dot{z_3}$.

We inject Eq. (19) and Eq. (17) in the previous expression:

$$\dot{V_3} = -\sum_{i=1}^{2} c_i{z_i}^2 + z_3[\beta_2 z_2 + \varphi_3(x) + \psi_3 u - \dot{\sigma_2}] \quad (20)$$

with $[\beta_2 z_2 + \varphi_3(x) + \psi_3 u - \dot{\sigma_2}] = -c_2 z_2$

We are able to design the control law u ensuring $\dot{V_3} \leq 0$.

$$u = \frac{-c_3 z_3 - \beta_2 z_2 - \varphi_3(x) + \dot{\sigma_2}}{\psi_3(x)} \qquad \psi_3(x) > 0$$

where c_3 is positive constant. Substituting β_2 and β_3 by their expression we have:

$$u = {T'}_{do}\frac{{x'}_{ds}}{V_s}\frac{-c_3 z_3 + \frac{\omega_S}{M}z_2 - \varphi_3(x) + \dot{\sigma_2}}{\sin x_1} \quad 0 < x_1 < \frac{\pi}{2} \quad (21)$$

$\dot{\sigma_2}$ is given by equation Eq. (16). Positives constant c_i is the tuning parameters of the nonlinear controller and $\varphi_3(x)$ is the nonlinear function resulting from the third equation of the nonlinear system Eq. (2).

CONCLUSION OF STEP 3

So, the time derivate of V_3 becomes:

$$\dot{V_3} = -\sum_{i=1}^{3} c_i{z_i}^2 \leq 0$$

CONCLUSION

The stability criterion of LYAPUNOV leads to $\lim_{t\to\infty}(z_1, z_2, z_3) \to 0$ – Fig 3a. This results in, $x_1 = \delta \to \delta_{ref}$, $x_2 = \omega \to 0$ and $x_1 = P_e \to P_m$. This last convergence implies the convergence of V_t toward V_s. Then we have just shown that the control law satisfies the convergence objectives given in the Section III.

V. SIMULATION RESULTS

Generator dynamics connected to the high power grid was simulated using MATLAB®R2016b with Simulink® environment.

5.1.TUNING PARAMETERS

We performed the simulations with synchronous generator parameters given in [3-5]. Controllers tuning parameters are given in Table 2.

TABLE 2, CONTROLLERS TUNING PARAMETERS

Backstepping	AVR-PSS
$c_1 = 1$ $c_2 = 10$ $c_3 = 0.5$	$K_A = 500$ $K_{PSS} = 0.5$ $T_W = 10s$ $T_1 = 0.2s$ $T_2 = 0.1s$ $T_R = 0$

5.2. ROBUSTNESS TEST

Our system will be tested by the following robustness test: combination of a short circuit on the transmission line lasting 500 *ms* occurring at 40 *s* after generator start-up and a

permanent drop of the mechanical power of 50% of its nominal value occurring 80 *s* after the start of the generator.

5.3. DISCUSSION

Temporal responses show that the implemented nonlinear regulator, called BCKSTP, gives satisfactory results. The AVR-PSS linear regulator ensures a good tracking of the reference trajectories. However, with the linear regulator, transient overrun appears in the dynamic of the power angle - Fig. 3c- while with the nonlinear regulator we can easily damp this transient overrun and improve the quickness of the dynamics of δ by playing on the parameter c_i. We note that during the short circuit, playing on these same parameters – Fig. 3e and Fig. 3f – can reduce the peaks of voltages and powers in transient state. After a mechanical power drop, the power angle does not return to its reference value since δ_{ref} depends on P_m in the expression Eq. (4) – Fig. 3c. The equilibrium point of the power angle has changed but remains stable because $0 < \delta < \frac{\pi}{2}$. Hence, the generator will not be subject to stall phenomena and the network will remain stable. We can see that the dynamics of ω regulated by our nonlinear controller reject the mechanical disturbance more quickly than the AVR-PSS regulator – Fig. 3d. The major disadvantage of the AVR-PSS is that the power has transient overrun and a peak overshoot during the short circuit – Fig. 3e. The control voltage of the BCKSTP regulator is smoother compared to the AVR-PSS signal – Fig. 3b. Indeed, a too high value of the gain of the voltage regulator K_A of the AVR-PSS regulator needed to obtain the convergence of V_t toward V_s degrades the control signal while the BCKSTP regulator does not have this disadvantage.

VI. CONCLUSION AND PERSPECTIVES

In this paper, a nonlinear backstepping control has been developed for synchronous generator excitation driven by tidal stream turbine. This proposed nonlinear controller regulates simultaneously terminal voltage and frequency making possible direct connection to electrical grid. Numerical results show a better convergence, reliability, transient stability and robustness compared to AVR-PSS. Indeed, the nonlinear controller designed with nonlinear equations system avoids a degradation of dynamics in transient and steady states with respect to a classical linear regulator. Soon, our research will focus on simulations and implementations of robust nonlinear controllers in multimachine configuration in order to anticipate tidal stream generators production parks development.

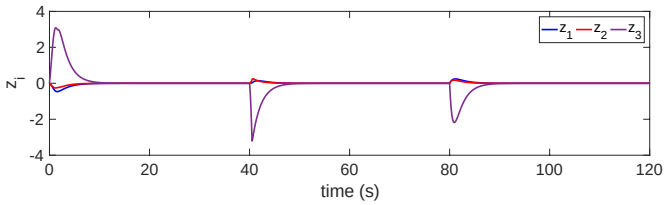

Fig 3a, Errors variables

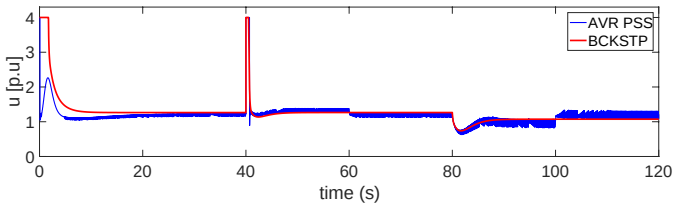

Fig 3b, Control signal

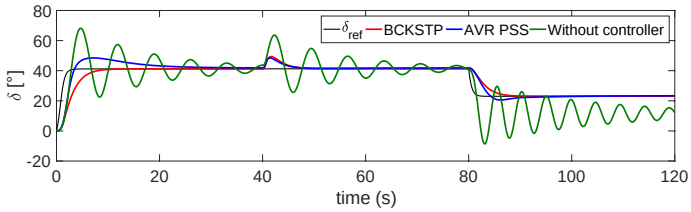

Fig 3c, Rotor angle

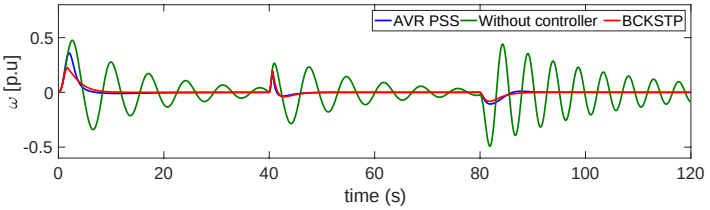

Fig 3d, Relative angular speed

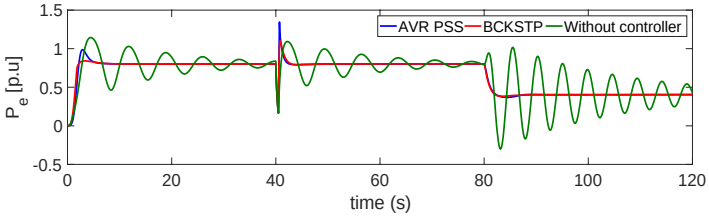

Fig 3e, Active electrical power

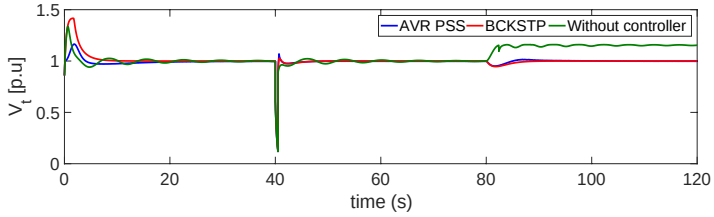

Fig 3d, Terminal voltage

REFERENCES

[1] S. Ben Elghali, M. Benbouzid, J. Charpentier, "Marine tidal current electric power generation technology : state of the art and current status", *IEEE electric machines and drives conference,* **2**, pp. 1407– 1412, 2007.

[2] F.P. Demello, C. Concordia, "Concepts of synchronous machine stability as affected by excitation control", *IEEE Trans. On Power Apparatus and System,* **88**, pp. 316-329, 1969.

[3] M. Dansoko, H. Nkwawo, B. Diourté, F. Floret, R. Goma, G. Kenné, "Decentralized sliding mode control for marine turbines connected to grid", *IFAC Internation Workshop on Adaptation and Learning in Control and Signal Processing,* **11**, pp. 3-5, 2013.

[4] M. Dansoko, H. Nkwawo, B. Diourté, F. Floret, R. Goma, G. Kenné, "Robust multivariable sliding mode control design for generator excitation of marine turbine in multimachine configuration", *Electrical Power and Energy System,* **63**, pp. 423-428, 2014.

[5] M. Dansoko, "Modeling and nonlinear control of marine turbines connected to an electrical network", *Thesis*, North Paris XIII Sorbonne University, 2014.

[6] Y. Wang, D. J. Hill, R. H. Middleton, L. Gao, "Transient stabilization of power systems with an adaptive control law", *Automatica,* **30**, pp. 1409-1413, 1994.

[7] G. Kenné, R. Goma, F. Lamnabhi-Lagarrigue, H. Nkwawo, A. Arzandé, J. C. Vannier, "An improved direct feedback linearization technique for transient stability enhancement and voltage regulation of power generators", *Electrical Power and Energy Systems,* **32**, pp. 809-816, 2010.

[8] P. W. Sauer, M. Pai, *Power System Dynamics and Stability*, Stipes Publishing L.L.C. University of Illinois at Urbana-Champaign, 1997.

[9] P. Anderson, A. Fouad, *Power System Stability and Control*, 2nd Edition, IEEE Press, 2003.

[10] A. Feuer, A. S. Morse, "Adaptive control of single-input single-output linear systems", *IEEE Trans. Automat. Contr*., **23** pp. 557-569, 1978.

[11] M. Krstić, I. Kanellakopoulos, P. V. Kokotović, *Nonlinear and Adaptive Control Design*, John Wiley and Sons, Ltd, 1995.

[12] P. V. Kokotović, "The joy of feedback nonlinear and adaptive", *IEEE Control Systems*, pp. 7-17, 1992.

[13] J. Zhou, C. Wen, *Adaptive Backstepping Control of Uncertain Systems*, **372** of Lecture Notes in Control And Information Sciences, springer, p. 228, 2008.